Prospects for discovery and spin discrimination of Higgs portal DM and imposters at future colliders

Pyungwon Ko
(Korea Institute for Advanced Study)

MITP 2019, Mainz, Germnay
April 3, 2019

Contents

- Higgs portal singlet fermion/vector DM models :
  - EFT vs. renormalizable, gauge invariant, unitary models
  - GC gamma ray excess,
- Collider Signatures including the interference between the SM Higgs and dark Higgs
- DM searches @ ILC 500
- DM searches @ 100 TeV pp collider

Let us start with

Higgs portal (S,F,V) DM

Higgs portal DM models

$$\mathcal{L}_{\rm scalar} = \frac{1}{2}\partial_\mu S \partial^\mu S - \frac{1}{2} m_S^2 S^2 - \frac{\lambda_{HS}}{2} H^\dagger H S^2 - \frac{\lambda_S}{4} S^4$$

$$\mathcal{L}_{\rm fermion} = \overline{\psi}\left[i\gamma\cdot\partial - m_\psi\right]\psi - \frac{\lambda_{H\psi}}{\Lambda} H^\dagger H\ \overline{\psi}\psi$$

$$\mathcal{L}_{\rm vector} = -\frac{1}{4} V_{\mu\nu}V^{\mu\nu} + \frac{1}{2} m_V^2 V_\mu V^\mu + \frac{1}{4}\lambda_V (V_\mu V^\mu)^2 + \frac{1}{2}\lambda_{HV} H^\dagger H V_\mu V^\mu .$$

All invariant under ad hoc Z2 symmetry

arXiv:1112.3299, … 1402.6287, etc.

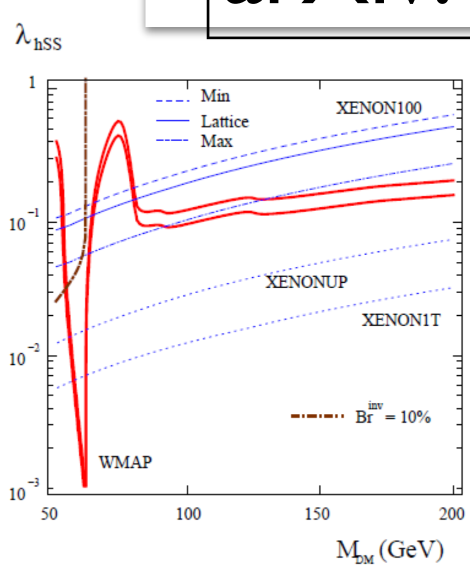

FIG. 1. Scalar Higgs-portal parameter space allowed by WMAP (between the solid red curves), XENON100 and $\mathrm{BR}^{\rm inv} = 10\%$ for $m_h = 125$ GeV. Shown also are the prospects for XENON upgrades.

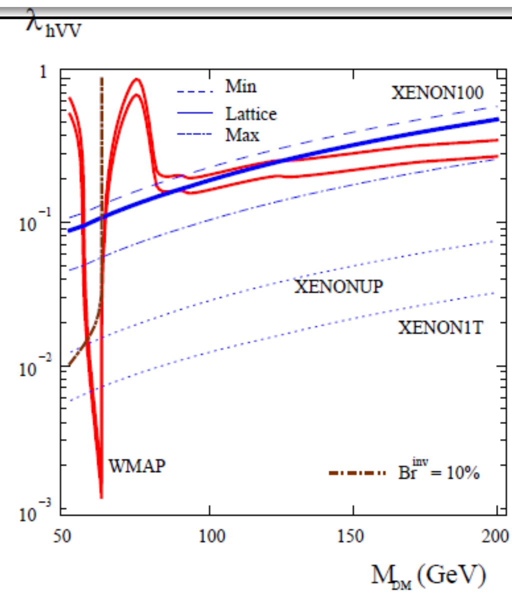

FIG. 2. Same as Fig. 1 for vector DM particles.

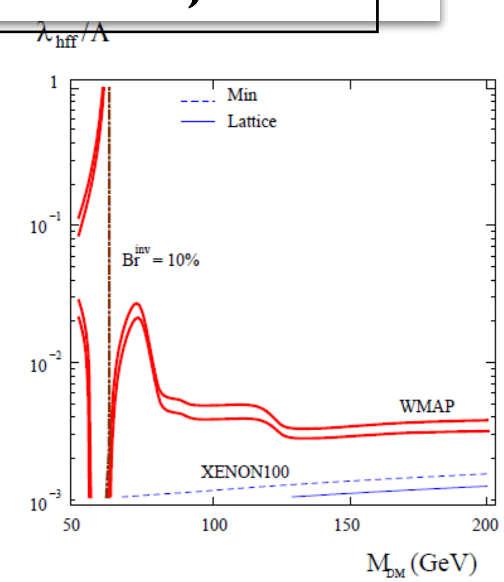

FIG. 3. Same as in Fig.1 for fermion DM; λ_{hff}/Λ is in GeV^{-1}.

Higgs portal DM models

$$\mathcal{L}_{\rm scalar} = \frac{1}{2}\partial_\mu S \partial^\mu S - \frac{1}{2} m_S^2 S^2 - \frac{\lambda_{HS}}{2} H^\dagger H S^2 - \frac{\lambda_S}{4} S^4$$

$$\mathcal{L}_{\rm fermion} = \overline{\psi}\left[i\gamma\cdot\partial - m_\psi\right]\psi - \frac{\lambda_{H\psi}}{\Lambda} H^\dagger H\ \overline{\psi}\psi$$

$$\mathcal{L}_{\rm vector} = -\frac{1}{4} V_{\mu\nu} V^{\mu\nu} + \frac{1}{2} m_V^2 V_\mu V^\mu + \frac{1}{4}\lambda_V (V_\mu V^\mu)^2 + \frac{1}{2}\lambda_{HV} H^\dagger H V_\mu V^\mu .$$

All invariant under ad hoc Z2 symmetry

- Scalar CDM : looks OK, renorm. .. BUT .....
- Fermion CDM : nonrenormalizable
- Vector CDM : looks OK, but it has a number of problems (in fact, it is not renormalizable)

Usual story within EFT

- Strong bounds from direct detection exp's put stringent bounds on the Higgs coupling to the dark matters
- So, the invisible Higgs decay is suppressed
- There is only one SM Higgs boson with the signal strengths equal to ONE if the invisible Higgs decay is ignored
- All these conclusions are not reproduced in the full theories (renormalizable) however

Singlet fermion CDM

Baek, Ko, Park, arXiv:1112.1847

$$\begin{aligned}\mathcal{L} &= \mathcal{L}_{\rm SM} - \mu_{HS} S H^\dagger H - \frac{\lambda_{HS}}{2} S^2 H^\dagger H \\ &+ \frac{1}{2}(\partial_\mu S \partial^\mu S - m_S^2 S^2) - \mu_S^3 S - \frac{\mu_S'}{3} S^3 - \frac{\lambda_S}{4} S^4 \\ &+ \overline{\psi}(i \not{\partial} - m_{\psi_0})\psi - \lambda S \overline{\psi}\psi\end{aligned}$$

mixing

invisible decay

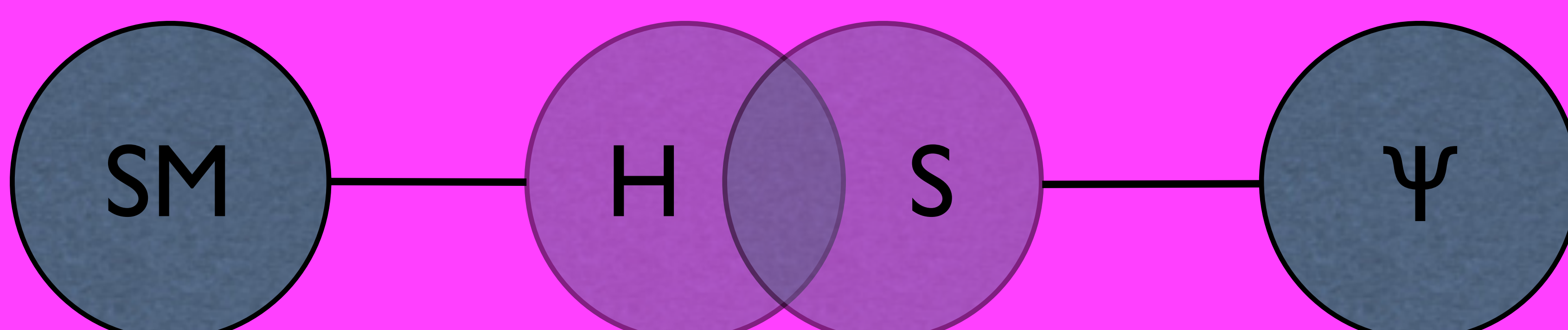

Production and decay rates are suppressed relative to SM.

This simple model has not been studied properly !!

Ratiocination

- Mixing and Eigenstates of Higgs-like bosons

$$\mu_H^2 = \lambda_H v_H^2 + \mu_{HS} v_S + \frac{1}{2}\lambda_{HS} v_S^2,$$
$$m_S^2 = -\frac{\mu_S^3}{v_S} - \mu_S' v_S - \lambda_S v_S^2 - \frac{\mu_{HS} v_H^2}{2v_S} - \frac{1}{2}\lambda_{HS} v_H^2,$$

at vacuum

$$M^2_{\text{Higgs}} \equiv \begin{pmatrix} m_{hh}^2 & m_{hs}^2 \\ m_{hs}^2 & m_{ss}^2 \end{pmatrix} \equiv \begin{pmatrix} \cos\alpha & \sin\alpha \\ -\sin\alpha & \cos\alpha \end{pmatrix} \begin{pmatrix} m_1^2 & 0 \\ 0 & m_2^2 \end{pmatrix} \begin{pmatrix} \cos\alpha & -\sin\alpha \\ \sin\alpha & \cos\alpha \end{pmatrix}$$

$$H_1 = h\cos\alpha - s\sin\alpha,$$
$$H_2 = h\sin\alpha + s\cos\alpha.$$

Mixing of Higgs and singlet

Ratiocination

- Signal strength (reduction factor)

$$r_i = \frac{\sigma_i \, \mathrm{Br}(H_i \to \mathrm{SM})}{\sigma_h \, \mathrm{Br}(h \to \mathrm{SM})}$$

$$r_1 = \frac{\cos^4\alpha \, \Gamma_{H_1}^{\mathrm{SM}}}{\cos^2\alpha \, \Gamma_{H_1}^{\mathrm{SM}} + \sin^2\alpha \, \Gamma_{H_1}^{\mathrm{hid}}}$$

$$r_2 = \frac{\sin^4\alpha \, \Gamma_{H_2}^{\mathrm{SM}}}{\sin^2\alpha \, \Gamma_{H_2}^{\mathrm{SM}} + \cos^2\alpha \, \Gamma_{H_2}^{\mathrm{hid}} + \Gamma_{H_2 \to H_1 H_1}}$$

$0 < \alpha < \pi/2 \Rightarrow r_1(r_2) < 1$

Invisible decay mode is not necessary!

If r_i > 1 for any single channel,
this model will be excluded !!

Constraints

- Dark matter to nucleon cross section (constraint)

$$\sigma_p \approx \frac{1}{\pi}\mu^2\lambda_p^2 \simeq 2.7\times 10^{-2}\frac{m_p^2}{\pi}\left|\left(\frac{m_p}{v}\right)\lambda \sin\alpha\cos\alpha\left(\frac{1}{m_1^2}-\frac{1}{m_2^2}\right)\right|^2$$

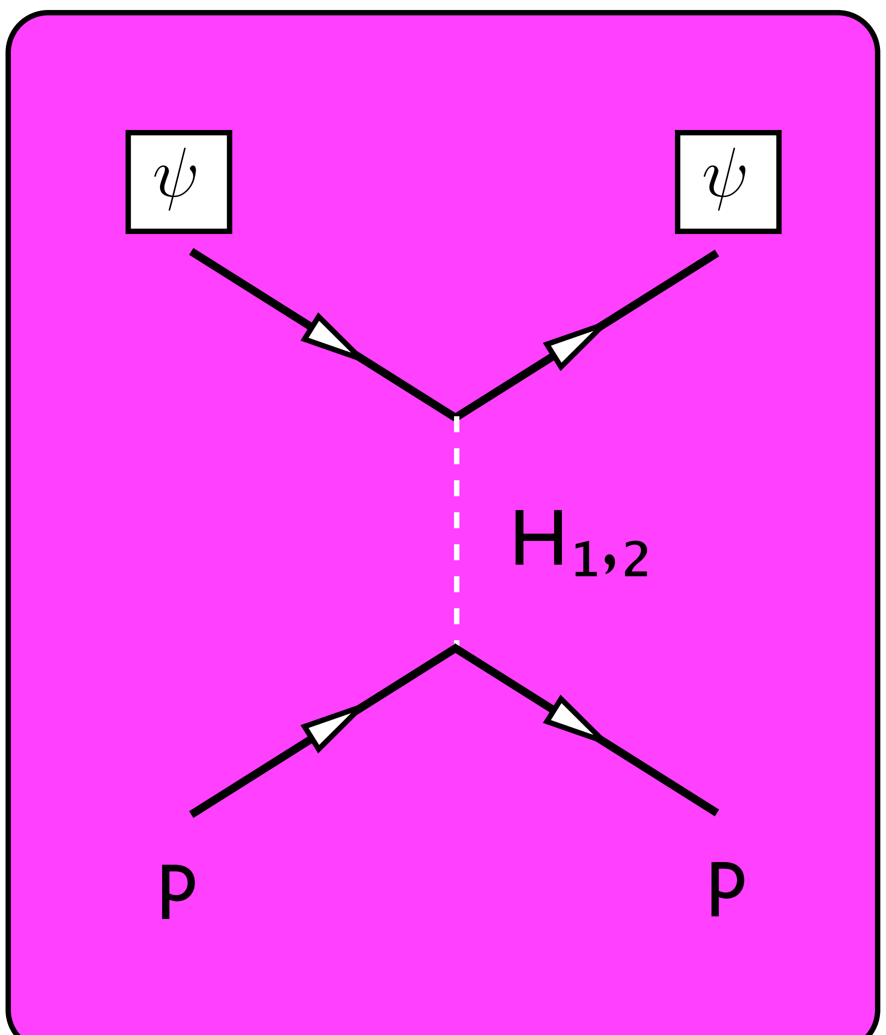

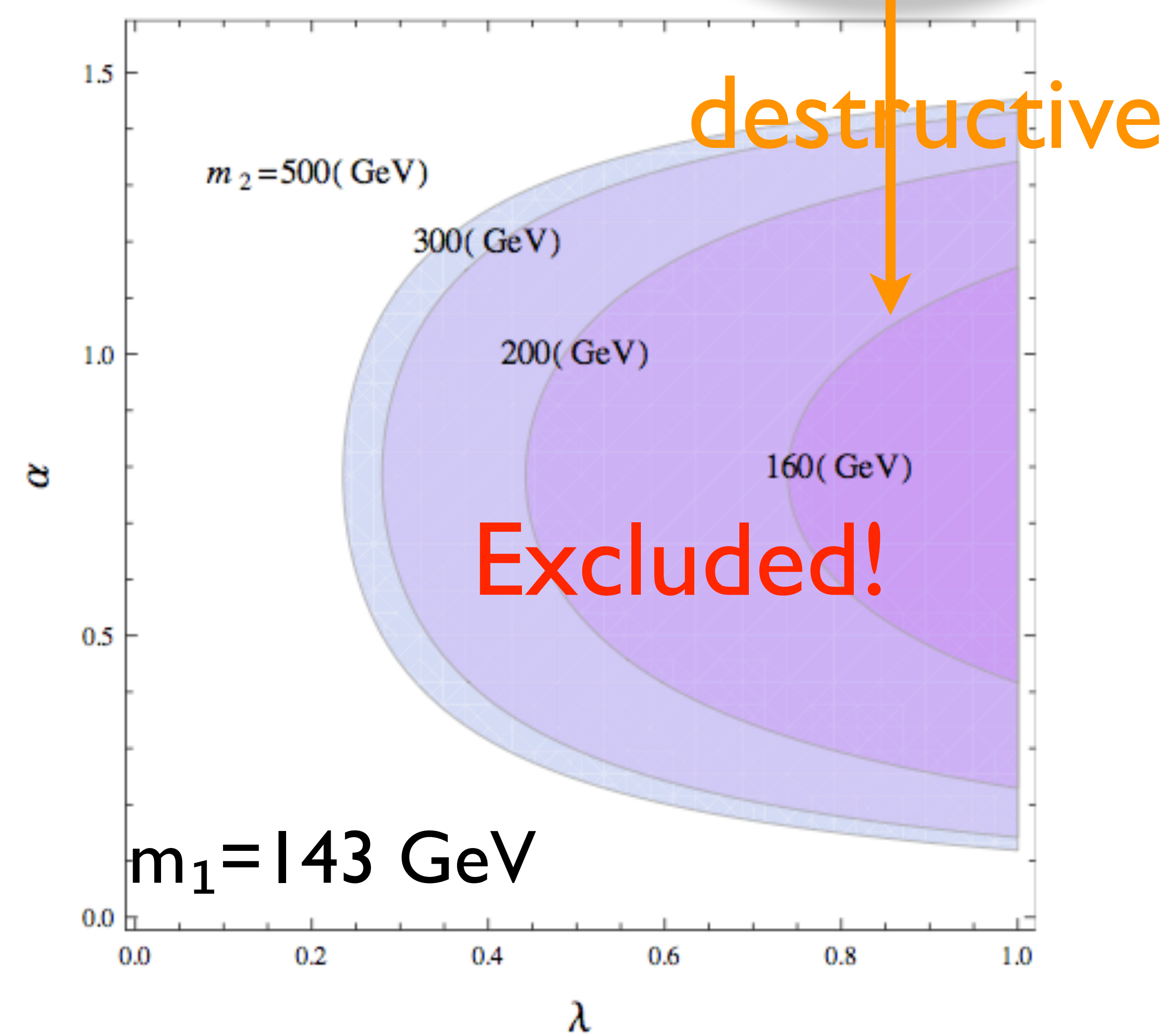

- We don’t use the effective lagrangian approach (nonrenormalizable interactions), since we don’t know the mass scale related with the CDM

$$\mathcal{L}_{\rm eff} = \overline{\psi}\left(m_0 + \frac{H^\dagger H}{\Lambda}\right)\psi. \qquad \text{or} \qquad \lambda h \overline{\psi}\psi$$

Breaks SM gauge sym

- Only one Higgs boson (alpha = 0)

- We cannot see the cancellation between two Higgs scalars in the direct detection cross section, if we used the above effective lagrangian

- The upper bound on DD cross section gives less stringent bound on the possible invisible Higgs decay

Low energy pheno.

- Universal suppression of collider SM signals

[See 1112.1847, Seungwon Baek, P. Ko & WIP]

- If "$m_h > 2\, m_\phi$", non-SM Higgs decay!

- Tree-level shift of $\lambda_{H,SM}$ (& loop correction)

$$\lambda_{\Phi H} \Rightarrow \lambda_H = \left[1 + \left(\frac{m_\phi^2}{m_h^2} - 1\right)\sin^2\alpha\right]\lambda_H^{\rm SM}$$

If "$m_\phi > m_h$", vacuum instability can be cured.

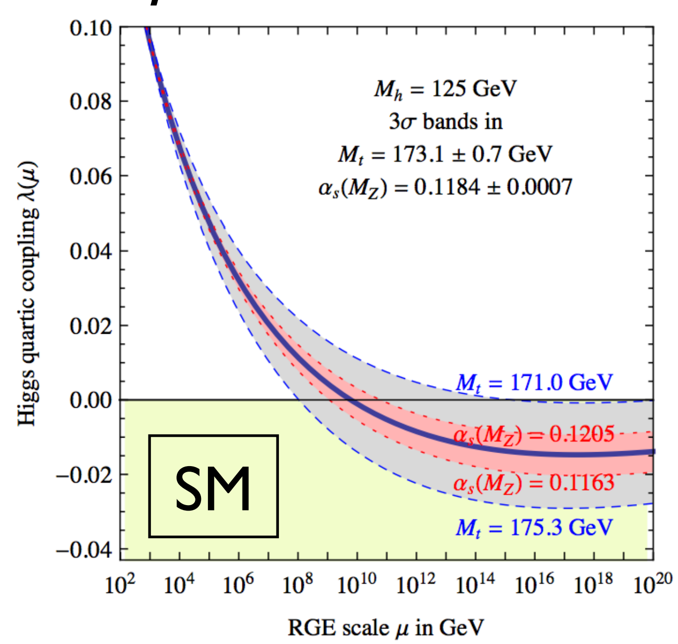

[G. Degrassi et al., 1205.6497]

α

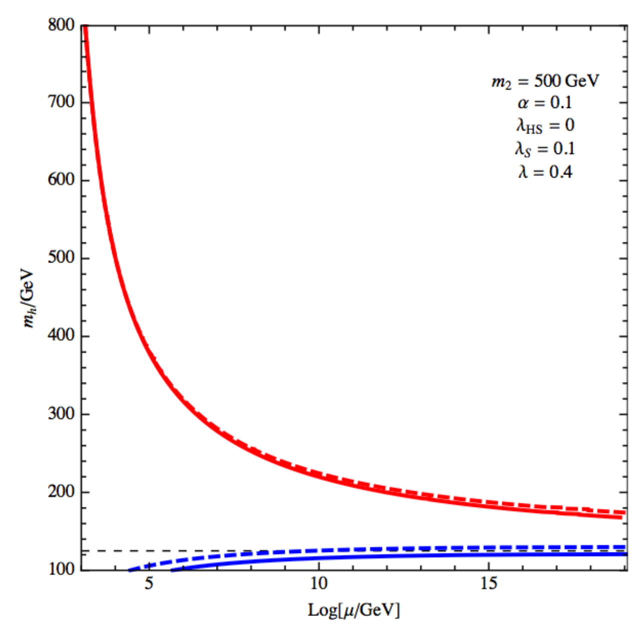

[S. Baek, P. Ko, WIP & E. Senaha, JHEP(2012)]

Vacuum Stability Improved by the singlet scalar S

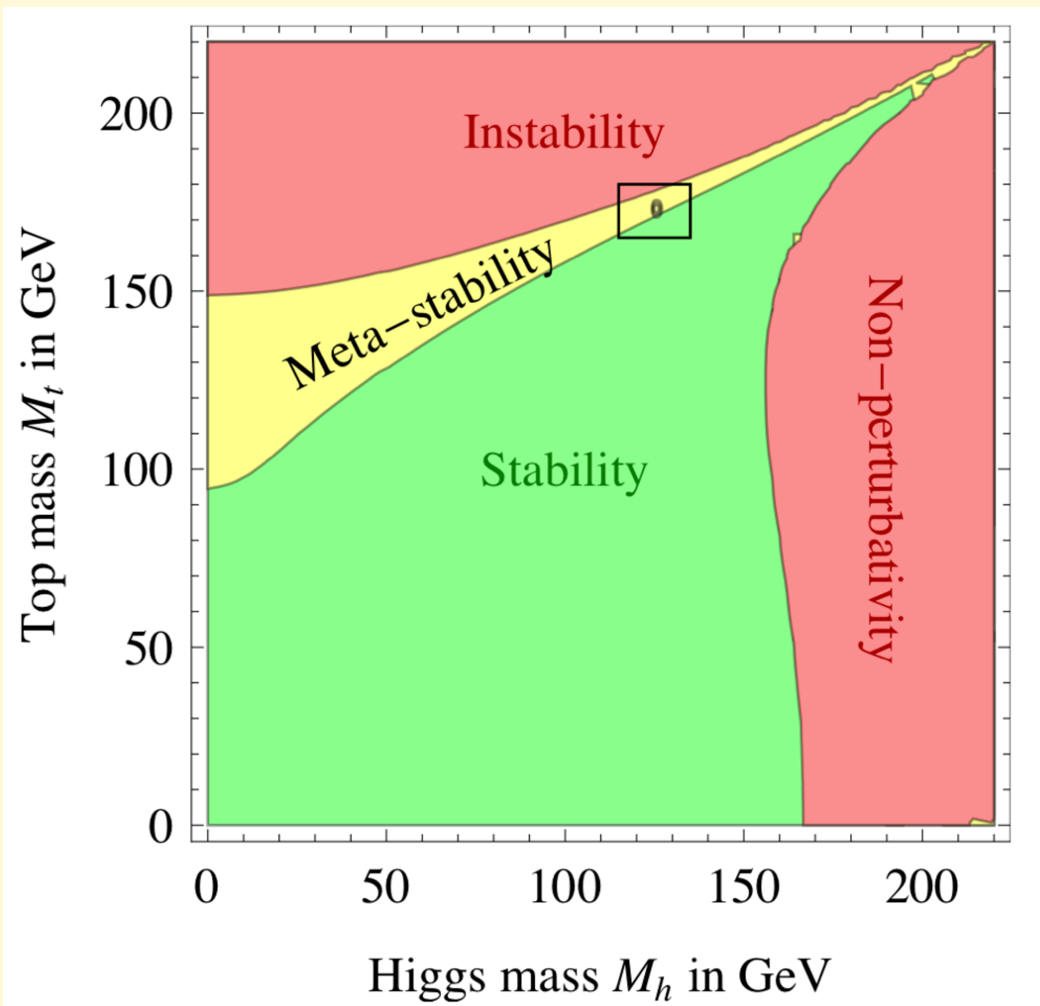

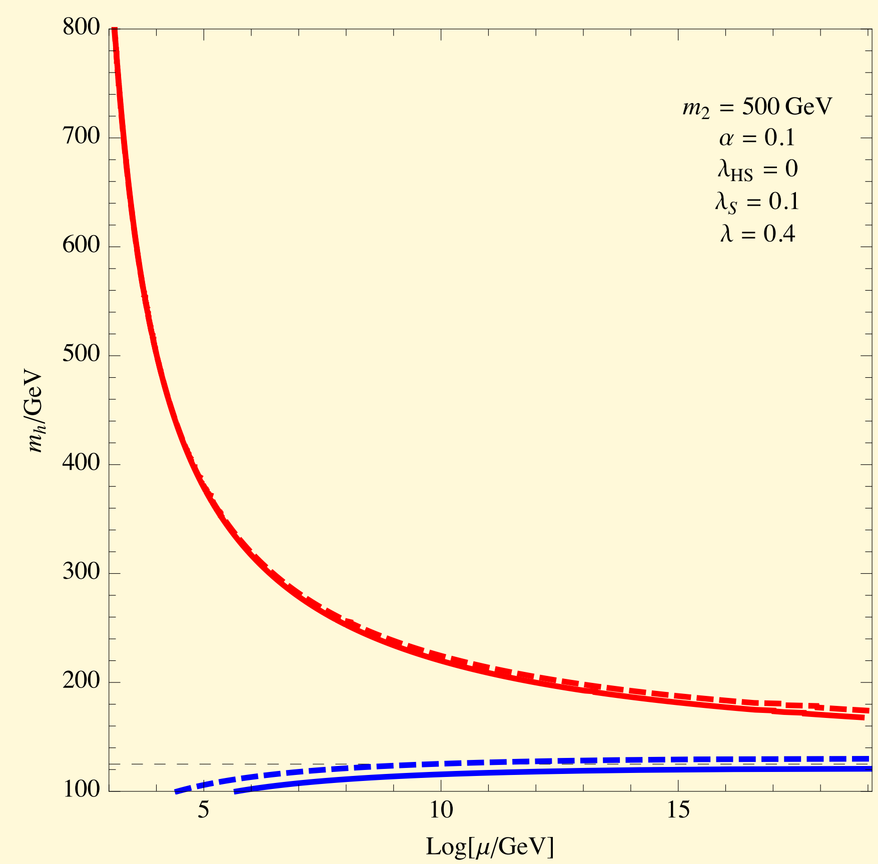

A. Strumia, Moriond EW 2013

Baek, Ko, Park, Senaha (2012)

Similar for Higgs portal Vector DM

$$\mathcal{L} = -m_V^2 V_\mu V^\mu - \frac{\lambda_{VH}}{4} H^\dagger H V_\mu V^\mu - \frac{\lambda_V}{4} (V_\mu V^\mu)^2$$

- Although this model looks renormalizable, it is not really renormalizable, since there is no agency for vector boson mass generation
- Need to a new Higgs that gives mass to VDM
- A complete model should be something like this:

$$\mathcal{L}_{VDM} = -\frac{1}{4}X_{\mu\nu}X^{\mu\nu} + (D_\mu\Phi)^\dagger(D^\mu\Phi) - \frac{\lambda_\Phi}{4}\left(\Phi^\dagger\Phi - \frac{v_\Phi^2}{2}\right)^2$$
$$-\lambda_{H\Phi}\left(H^\dagger H - \frac{v_H^2}{2}\right)\left(\Phi^\dagger\Phi - \frac{v_\Phi^2}{2}\right) \;,$$

$$\langle 0|\phi_X|0\rangle = v_X + h_X(x)$$

$X_\mu \equiv V_\mu$ here

- There appear a new singlet scalar h_X from phi_X , which mixes with the SM Higgs boson through Higgs portal

- The effects must be similar to the singlet scalar in the fermion CDM model, and generically true in the DM with dark gauge sym

- Important to consider a minimal renormalizable and unitary model to discuss physics correctly [Baek, Ko, Park and Senaha, arXiv: 1212.2131 (JHEP)]

- Can accommodate GeV scale gamma ray excess from GC

New scalar improves EW vacuum stability

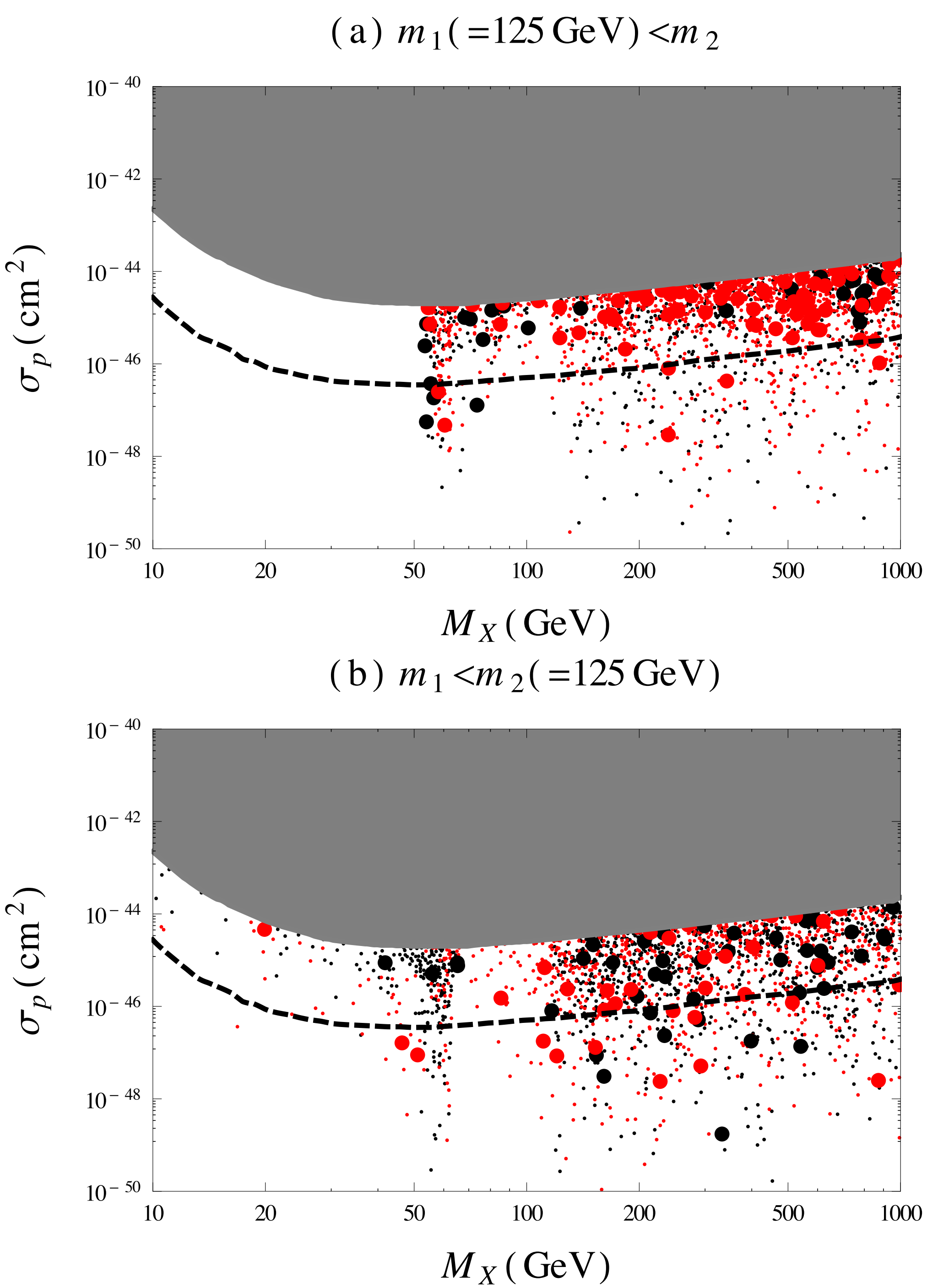

Figure 6. The scattered plot of σ_p as a function of M_X. The big (small) points (do not) satisfy the WMAP relic density constraint within 3 σ, while the red-(black-)colored points gives $r_1 > 0.7 (r_1 < 0.7)$. The grey region is excluded by the XENON100 experiment. The dashed line denotes the sensitivity of the next XENON experiment, XENON1T.

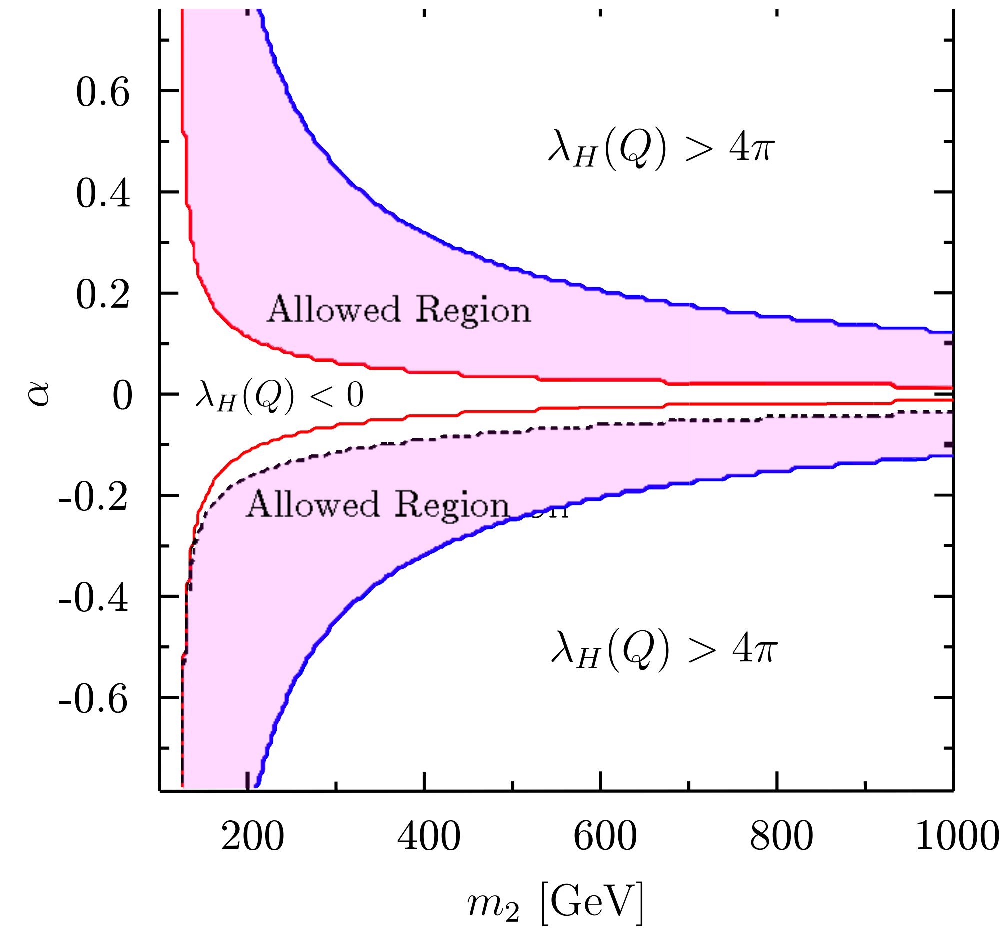

Figure 8. The vacuum stability and perturbativity constraints in the α-m_2 plane. We take $m_1 = 125$ GeV, $g_X = 0.05$, $M_X = m_2/2$ and $v_\Phi = M_X/(g_X Q_\Phi)$.

Higgs portal DM as examples

$$\mathcal{L}_{\rm scalar} = \frac{1}{2}\partial_\mu S \partial^\mu S - \frac{1}{2}m_S^2 S^2 - \frac{\lambda_{HS}}{2} H^\dagger H S^2 - \frac{\lambda_S}{4} S^4$$

$$\mathcal{L}_{\rm fermion} = \overline{\psi}\left[i\gamma\cdot\partial - m_\psi\right]\psi - \frac{\lambda_{H\psi}}{\Lambda} H^\dagger H \, \overline{\psi}\psi$$

$$\mathcal{L}_{\rm vector} = -\frac{1}{4}V_{\mu\nu}V^{\mu\nu} + \frac{1}{2}m_V^2 V_\mu V^\mu + \frac{1}{4}\lambda_V (V_\mu V^\mu)^2 + \frac{1}{2}\lambda_{HV} H^\dagger H V_\mu V^\mu .$$

All invariant under ad hoc Z2 symmetry

arXiv:1112.3299, … 1402.6287, etc.

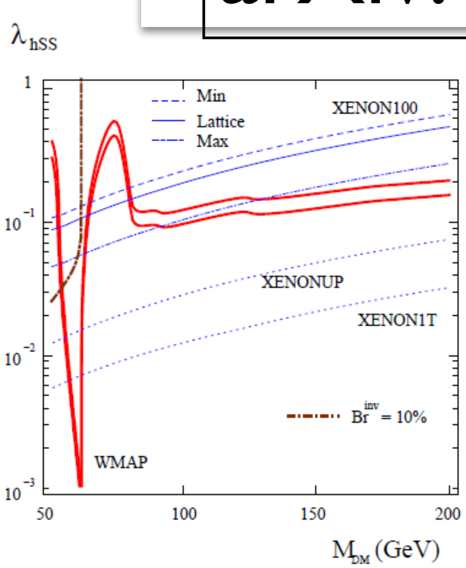

FIG. 1. Scalar Higgs-portal parameter space allowed by WMAP (between the solid red curves), XENON100 and $BR^{inv} = 10\%$ for $m_h = 125$ GeV. Shown also are the prospects for XENON upgrades.

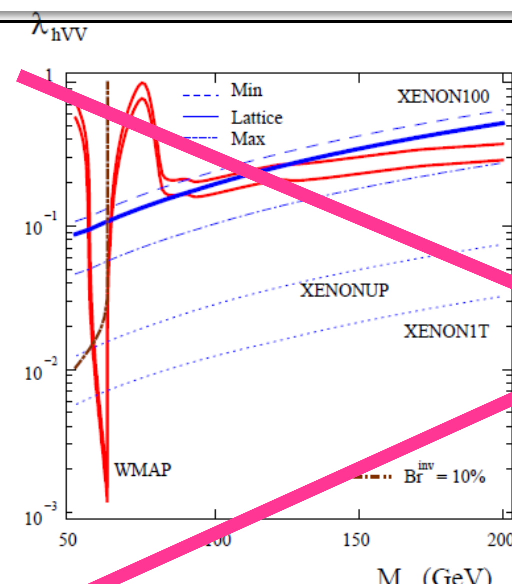

FIG. 2. Same as Fig. 1 for vector DM particles.

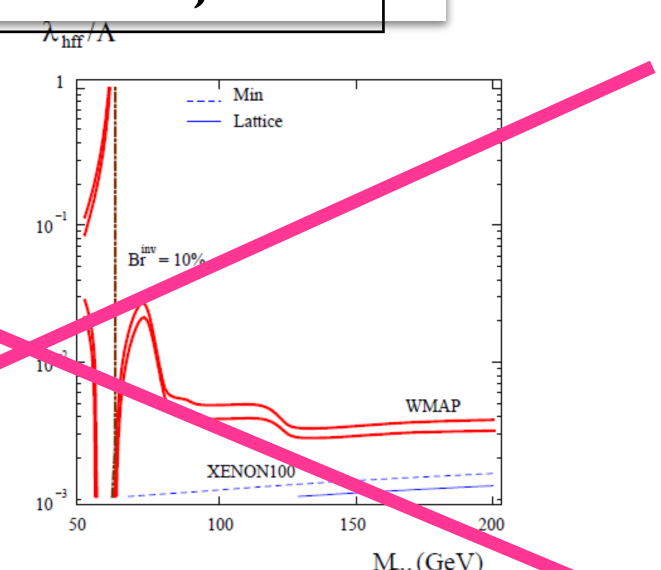

FIG. 3. Same as in Fig.1 for fermion DM; λ_{hff}/Λ is in GeV^{-1}.

Higgs portal DM as examples

$$\mathcal{L}_{\rm scalar} = \frac{1}{2}\partial_\mu S \partial^\mu S - \frac{1}{2} m_S^2 S^2 - \frac{\lambda_{HS}}{2} H^\dagger H S^2 - \frac{\lambda_S}{4} S^4$$

$$\mathcal{L}_{\rm fermion} = \overline{\psi}\left[i\gamma\cdot\partial - m_\psi \right]\psi - \frac{\lambda_{H\psi}}{\Lambda} H^\dagger H \, \overline{\psi}\psi$$

$$\mathcal{L}_{\rm vector} = -\frac{1}{4} V_{\mu\nu}V^{\mu\nu} + \frac{1}{2} m_V^2 V_\mu V^\mu + \frac{1}{4}\lambda_V (V_\mu V^\mu)^2 + \frac{1}{2}\lambda_{HV} H^\dagger H V_\mu V^\mu .$$

All invariant under ad hoc Z2 symmetry

arXiv:1112.3299, … 1402.6287, etc.

We need to include dark Higgs (singlet scalar) to get renormalizable/unitary models for fermion or vector DM

FIG. 1. Scalar Higgs-portal parameter space allowed by WMAP (between the solid red curves), XENON100 and BR$^{\rm inv}$ = 10% for m_h = 125 GeV. Shown also are the prospects for XENON upgrades.

FIG. 2. Same as Fig. 1 for vector DM particles.

FIG. 3. Same as in Fig.1 for fermion DM; λ_{hff}/Λ is in GeV^{-1}.

Is this any useful in phenomenology ?

YES !

Fermi-LAT GC γ-ray excess

see arXiv:1612.05687 for a recent overview by C.Karwin, S. Murgia, T. Tait, T.A.Porter, P. Tanedo

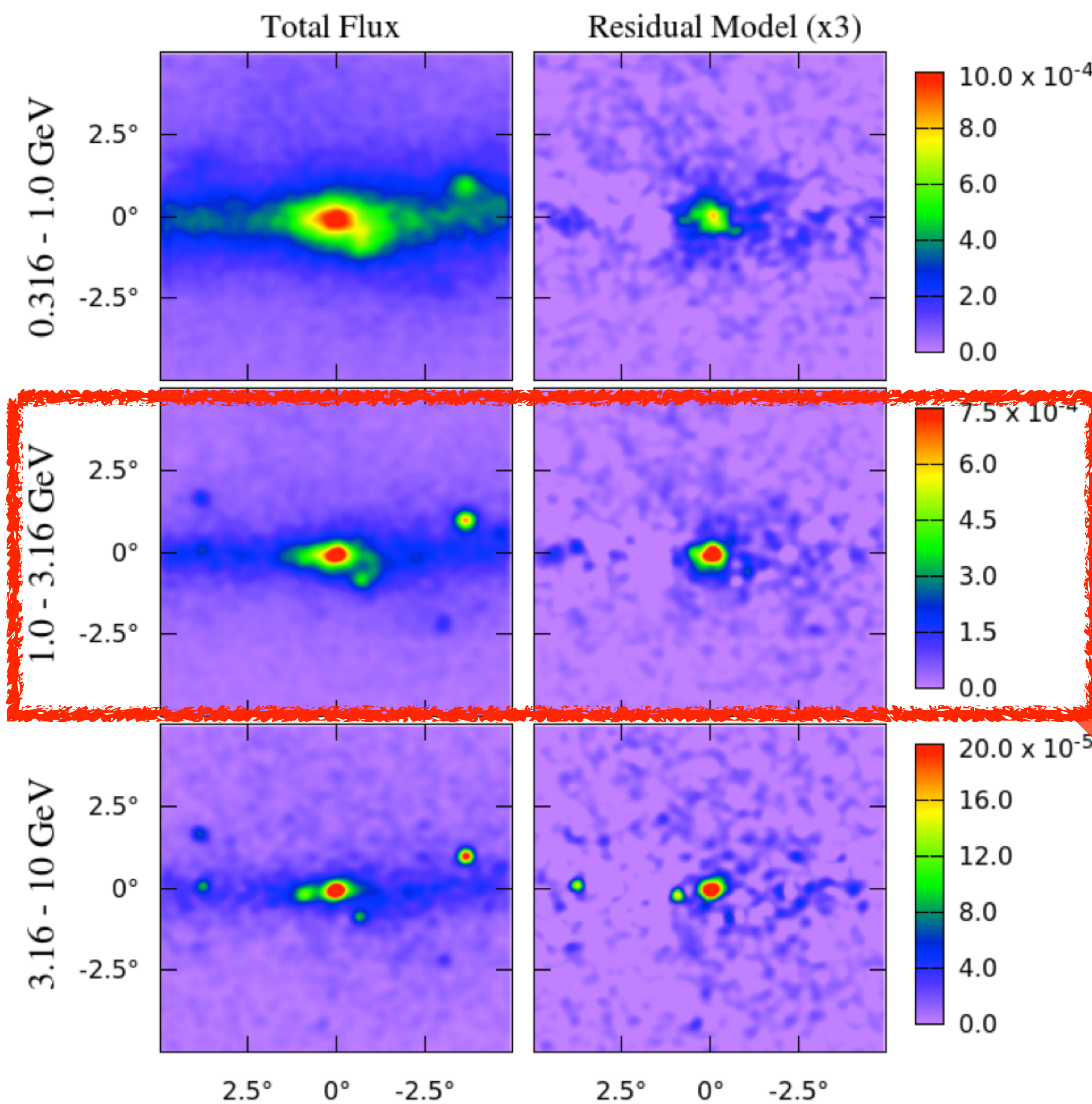

[1402.6703, T. Daylan et.al.]

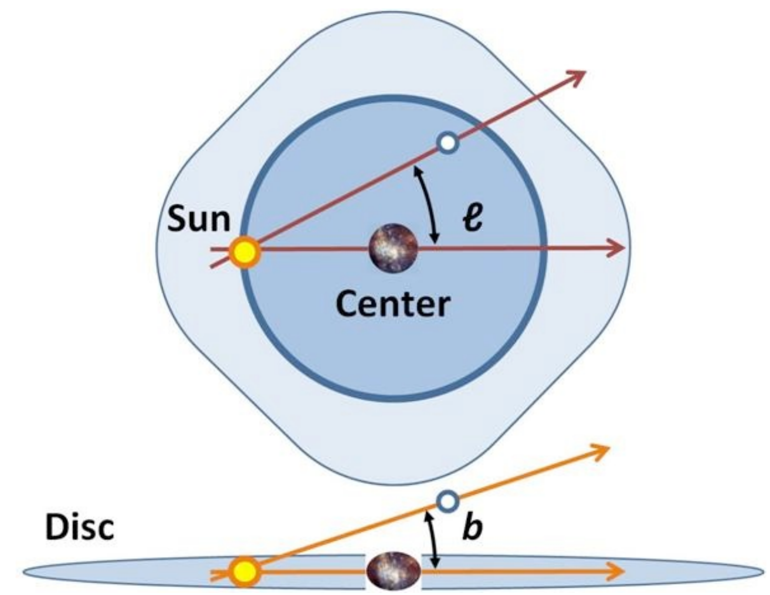

$$\mathrm{GC} : b \sim l \lesssim 0.1^\circ$$

extended

GeV scale excess!

- A DM interpretation

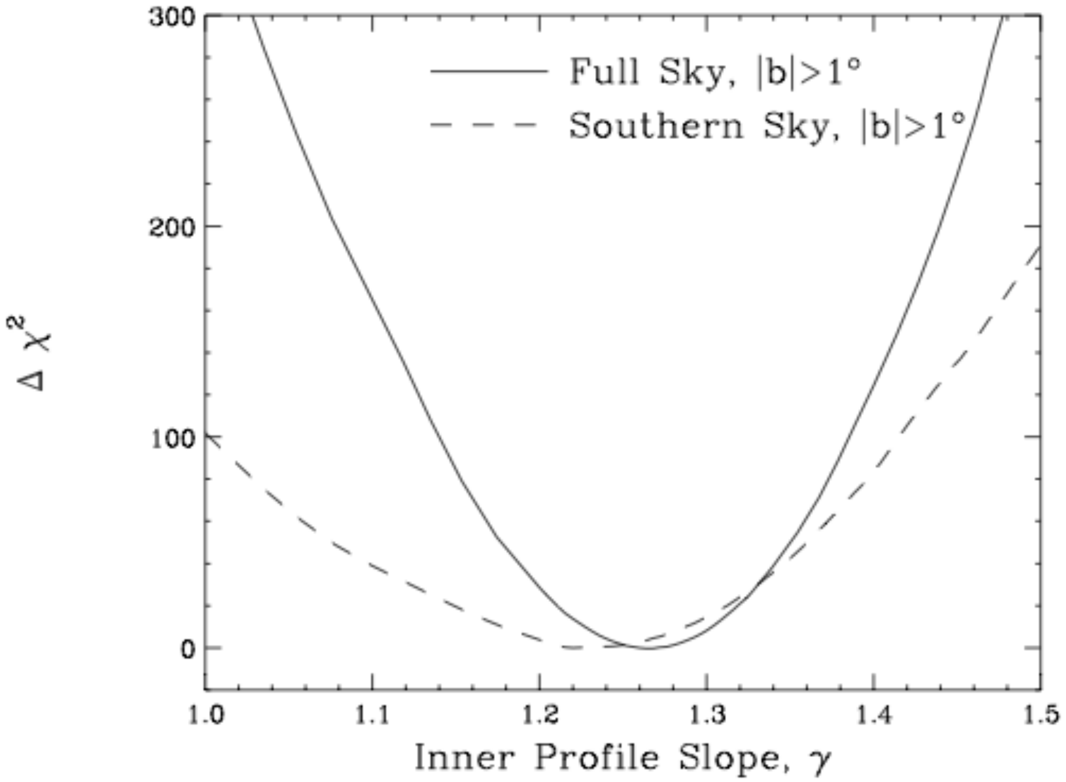

$\mathrm{DM} + \mathrm{DM} \to b\bar{b}$ with $\sigma v = 1.7 \times 10^{-26} \mathrm{cm}^3/\mathrm{s}$

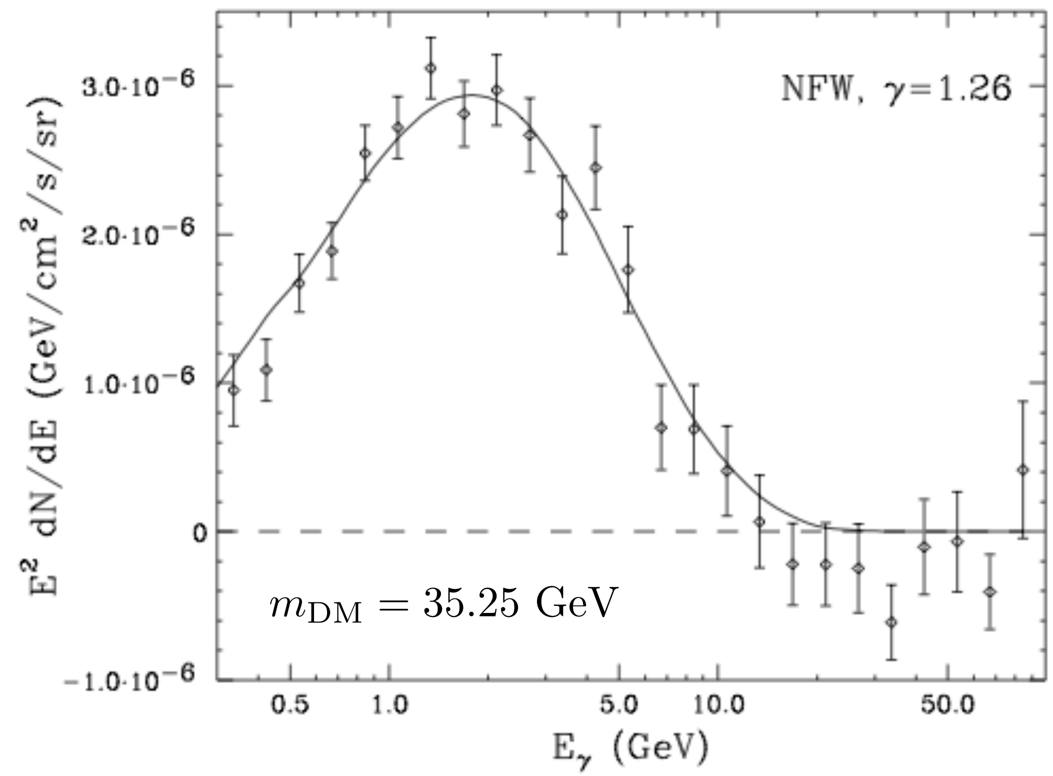

* See "1402.6703, T. Daylan et.al." for other possible channels

- Millisecond Pulars (astrophysical alternative)

It may or may not be the main source, depending on

- luminosity func.
- bulge population
- distribution of bulge population

* See "1404.2318, Q. Yuan & B. Zhang" and "1407.5625, I. Cholis, D. Hooper & T. Linden"

GC gamma ray in VDM

[1404.5257, P. Ko, WIP & Y. Tang] JCAP (2014)
(Also Celine Boehm et al. 1404.4977, PRD)

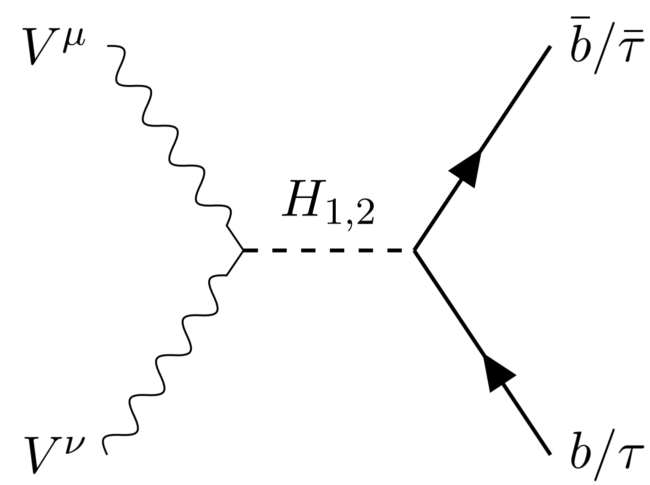

H2 : 125 GeV Higgs
H1 : absent in EFT

Figure 2. Dominant s channel $b + \bar{b}$ (and $\tau + \bar{\tau}$) production

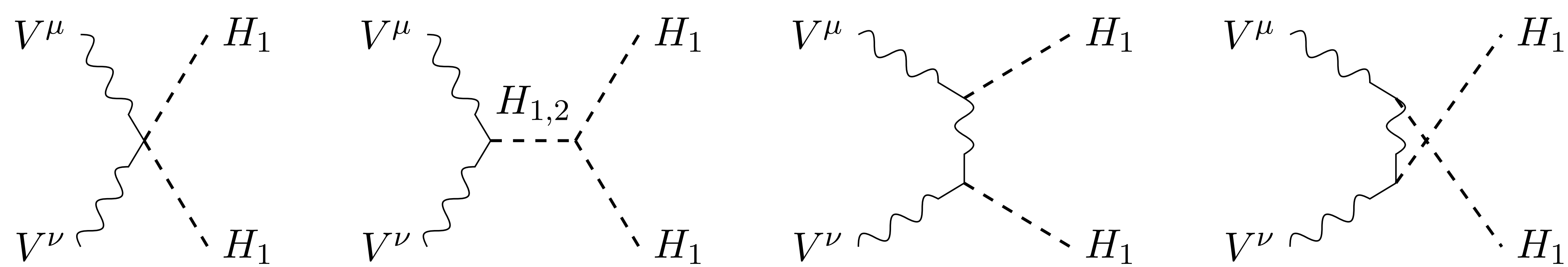

Figure 3. Dominant s/t-channel production of H_1s that decay dominantly to $b + \bar{b}$

Importance of VDM with Dark Higgs Boson

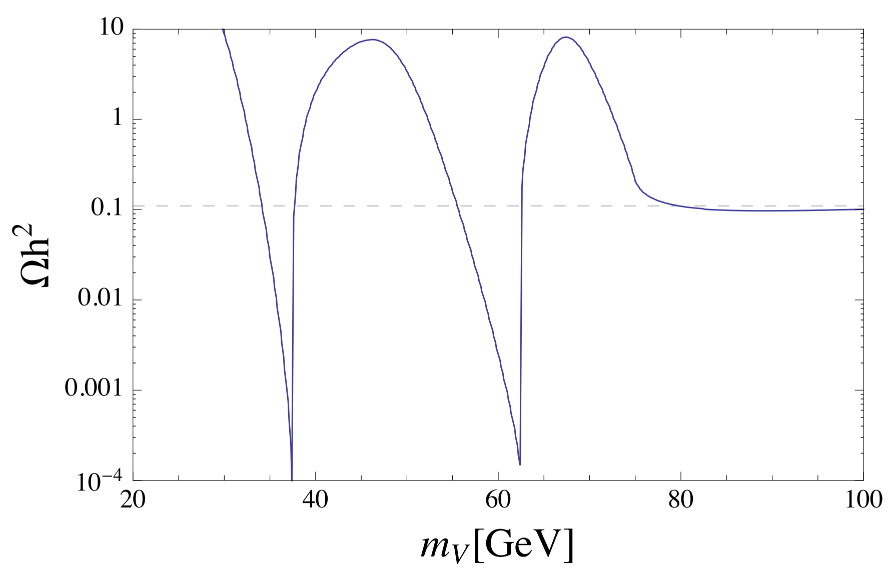

Figure 4. Relic density of dark matter as function of m_ψ for $m_h = 125$, $m_\phi = 75\,\text{GeV}$, $g_X = 0.2$, and $\alpha = 0.1$.

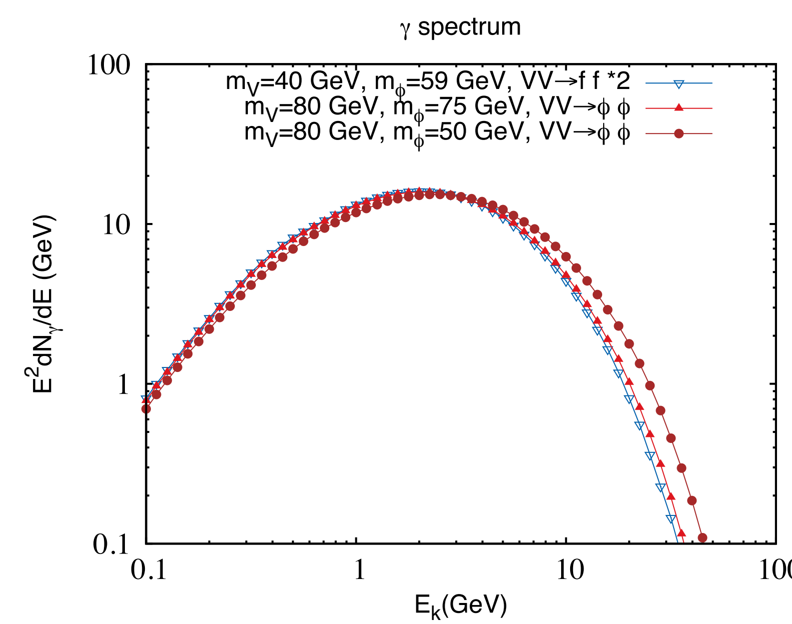

Figure 5. Illustration of γ spectra from different channels. The first two cases give almost the same spectra while in the third case γ is boosted so the spectrum is shifted to higher energy.

This mass range of VDM would have been impossible in the VDM model (EFT)

And No 2nd neutral scalar (Dark Higgs) in EFT

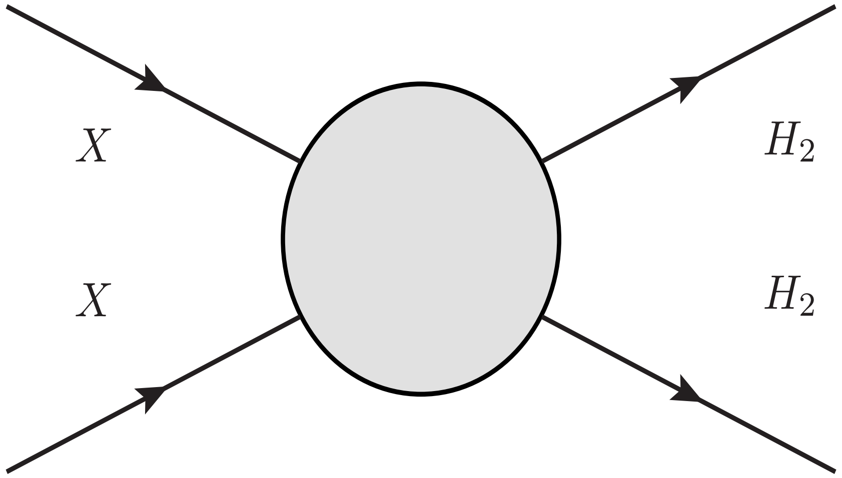

P.Ko, Yong Tang.
arXiv:1504.03908

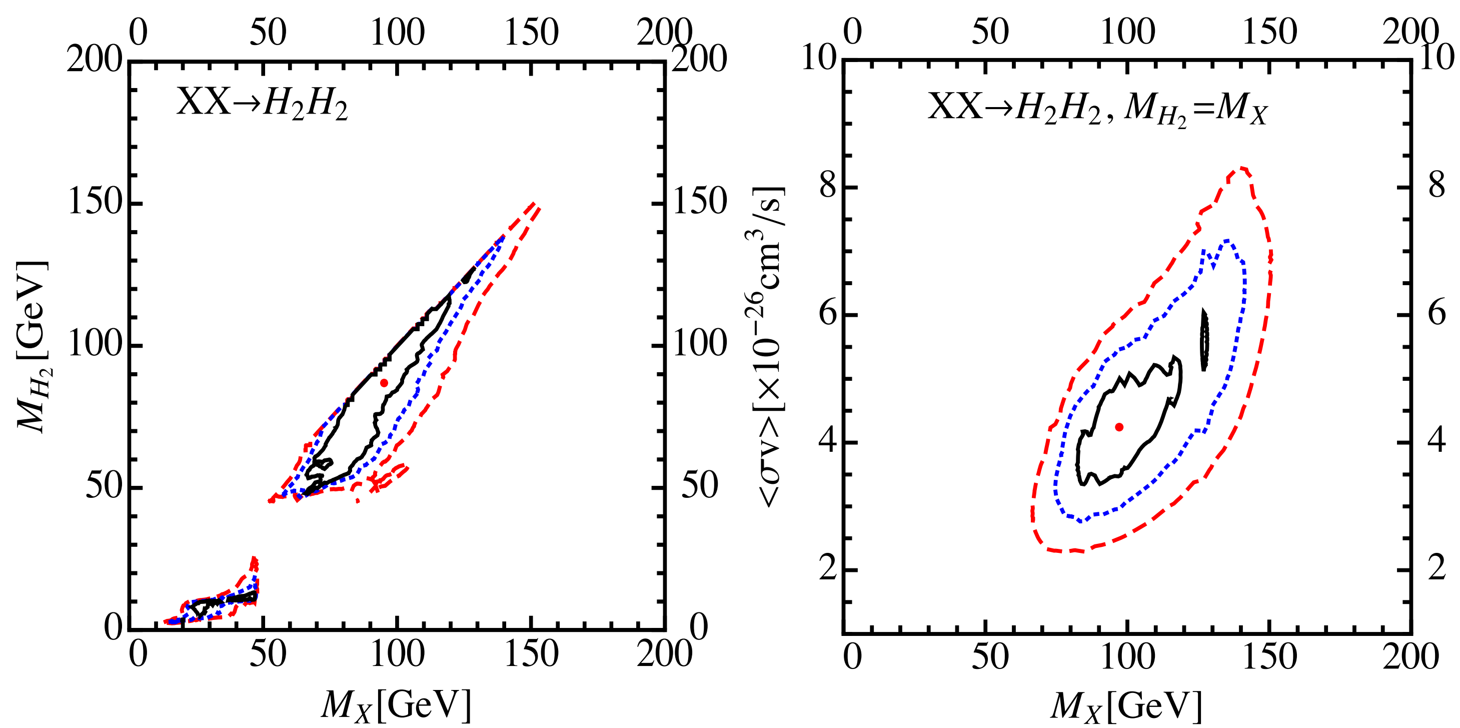

FIG. 3: The regions inside solid(black), dashed(blue) and long-dashed(red) contours correspond to 1σ, 2σ and 3σ, respectively. The red dots inside 1σ contours are the best-fit points. In the left panel, we vary freely M_X, M_{H_2} and $\langle\sigma v\rangle$. While in the right panel, we fix the mass of H_2, $M_{H_2} \simeq M_X$.

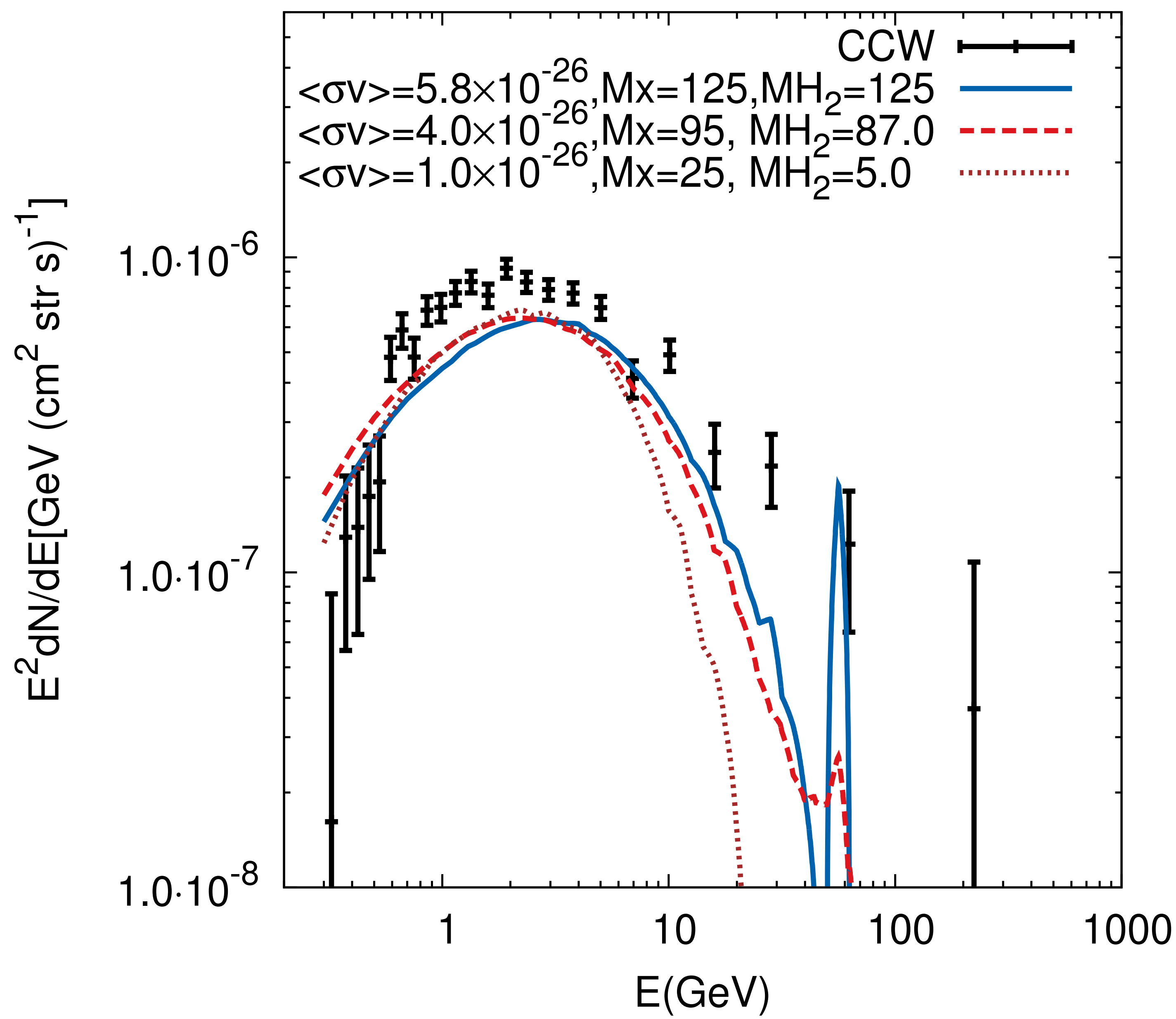

FIG. 2: Three illustrative cases for gamma-ray spectra in contrast with CCW data points [11]. All masses are in GeV unit and σv with cm^3/s. Line shape around $E \simeq M_{H_2}/2$ is due to decay modes, $H_2 \to \gamma\gamma, Z\gamma$.

This would have never been possible within the DM EFT

P.Ko, Yong Tang.
arXiv:1504.03908

Channels	Best-fit parameters	$\chi^2_{\rm min}/\text{d.o.f.}$	p-value
$XX \to H_2H_2$ (with $M_{H_2} \neq M_X$)	$M_X \simeq 95.0\text{GeV}, M_{H_2} \simeq 86.7\text{GeV}$ $\langle\sigma v\rangle \simeq 4.0 \times 10^{-26}\text{cm}^3/\text{s}$	$22.0/21$	0.40
$XX \to H_2H_2$ (with $M_{H_2} = M_X$)	$M_X \simeq 97.1\text{GeV}$ $\langle\sigma v\rangle \simeq 4.2 \times 10^{-26}\text{cm}^3/\text{s}$	$22.5/22$	0.43
$XX \to H_1H_1$ (with $M_{H_1} = 125\text{GeV}$)	$M_X \simeq 125\text{GeV}$ $\langle\sigma v\rangle \simeq 5.5 \times 10^{-26}\text{cm}^3/\text{s}$	$24.8/22$	0.30
$XX \to b\bar{b}$	$M_X \simeq 49.4\text{GeV}$ $\langle\sigma v\rangle \simeq 1.75 \times 10^{-26}\text{cm}^3/\text{s}$	$24.4/22$	0.34

TABLE I: Summary table for the best fits with three different assumptions.

Collider Implications

$m_h = 125\text{GeV},\ \text{Br}(H \to \text{inv}) < 0.51$ at 90% CL

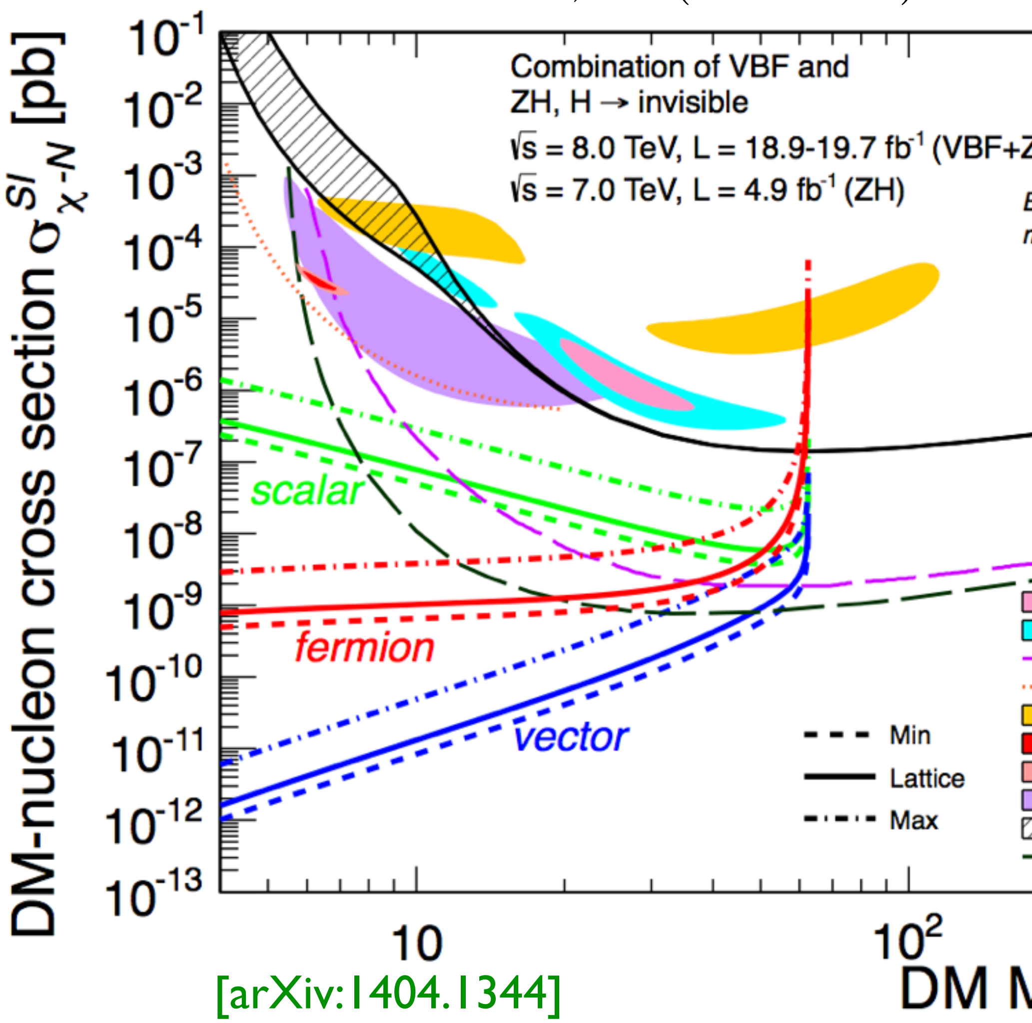

[arXiv:1404.1344]

Based on EFTs

$m_h = 125.5\text{GeV},\ \text{Br}(H \to \text{inv}) < 0.52$ at 90% CL

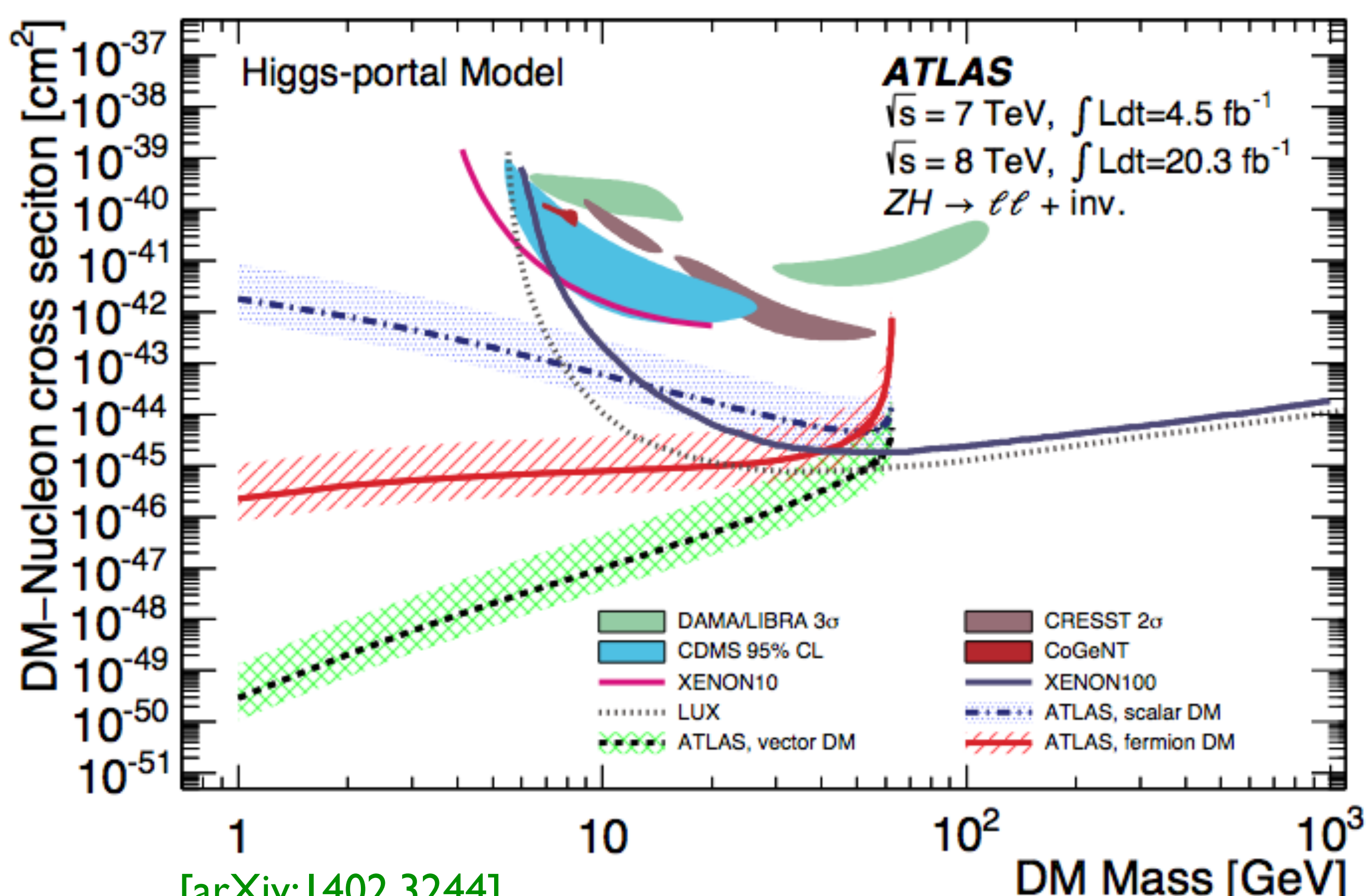

[arXiv:1402.3244]

- However, in renormalizable unitary models of Higgs portals, 2 more relevant parameters

[arXiv: 1405.3530, S. Baek, P. Ko & WIPark, PRD]

$$\mathcal{L}_{\rm SFDM} = \overline{\psi}\left(i\partial - m_\psi - \lambda_\psi S\right) - \mu_{HS} S H^\dagger H - \frac{\lambda_{HS}}{2} S^2 H^\dagger H + \frac{1}{2}\partial_\mu S \partial^\mu S - \frac{1}{2} m_S^2 S^2 - \mu_S^3 S - \frac{\mu_S'}{3} S^3 - \frac{\lambda_S}{4} S^4 .$$

$$\mathcal{L}_{\rm VDM} = -\frac{1}{4} V_{\mu\nu} V^{\mu\nu} + D_\mu \Phi^\dagger D^\mu \Phi - \lambda_\Phi \left(\Phi^\dagger \Phi - \frac{v_\Phi^2}{2}\right)^2 - \lambda_{\Phi H}\left(\Phi^\dagger\Phi - \frac{v_\Phi^2}{2}\right)\left(H^\dagger H - \frac{v_H^2}{2}\right)$$

$$\begin{aligned} \sigma_p^{\rm SI} &= (\sigma_p^{\rm SI})_{\rm EFT}\ c_\alpha^4 m_h^4 \mathcal{F}(m_{\rm DM}, \{m_i\}, v) \\ &\simeq (\sigma_p^{\rm SI})_{\rm EFT}\ c_\alpha^4 \left(1 - \frac{m_h^2}{m_2^2}\right)^2 \end{aligned}$$

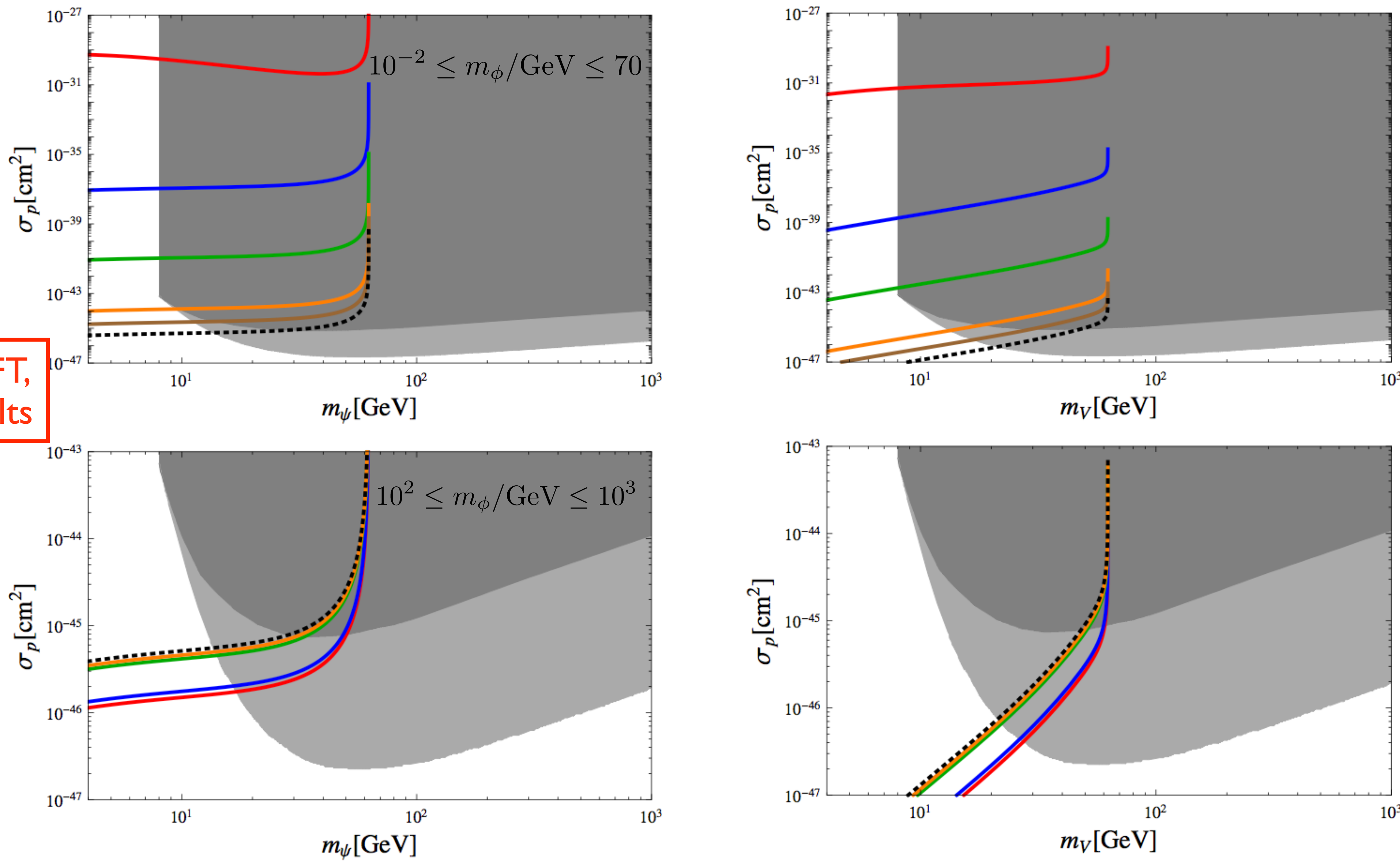

Dashed curves: EFT, ATLAS, CMS results

- However, in renormalizable unitary models of Higgs portals, 2 more relevant parameters

$$\mathcal{L}_{\rm SFDM} = \overline{\psi}\left(i\partial\!\!\!/ - m_\psi - \lambda_\psi S\right) - \mu_{HS} S H^\dagger H - \frac{\lambda_{HS}}{2} S^2 H^\dagger H + \frac{1}{2}\partial_\mu S \partial^\mu S - \frac{1}{2} m_S^2 S^2 - \mu_S^3 S - \frac{\mu_S'}{3} S^3 - \frac{\lambda_S}{4} S^4.$$

$$\sigma_p^{\rm SI} = (\sigma_p^{\rm SI})_{\rm EFT}\; c_\alpha^4 m_h^4 \mathcal{F}(m_{\rm DM}, \{m_i\}, v) \simeq (\sigma_p^{\rm SI})_{\rm EFT}\; c_\alpha^4 \left(1 - \frac{m_h^2}{m_2^2}\right)^2$$

$$\mathcal{L}_{\rm VDM} = -\frac{1}{4} V_{\mu\nu} V^{\mu\nu} + D_\mu \Phi^\dagger D^\mu \Phi - \lambda_\Phi \left(\Phi^\dagger \Phi - \frac{v_\Phi^2}{2}\right)^2 - \lambda_{\Phi H} \left(\Phi^\dagger \Phi - \frac{v_\Phi^2}{2}\right)\left(H^\dagger H - \frac{v_H^2}{2}\right)$$

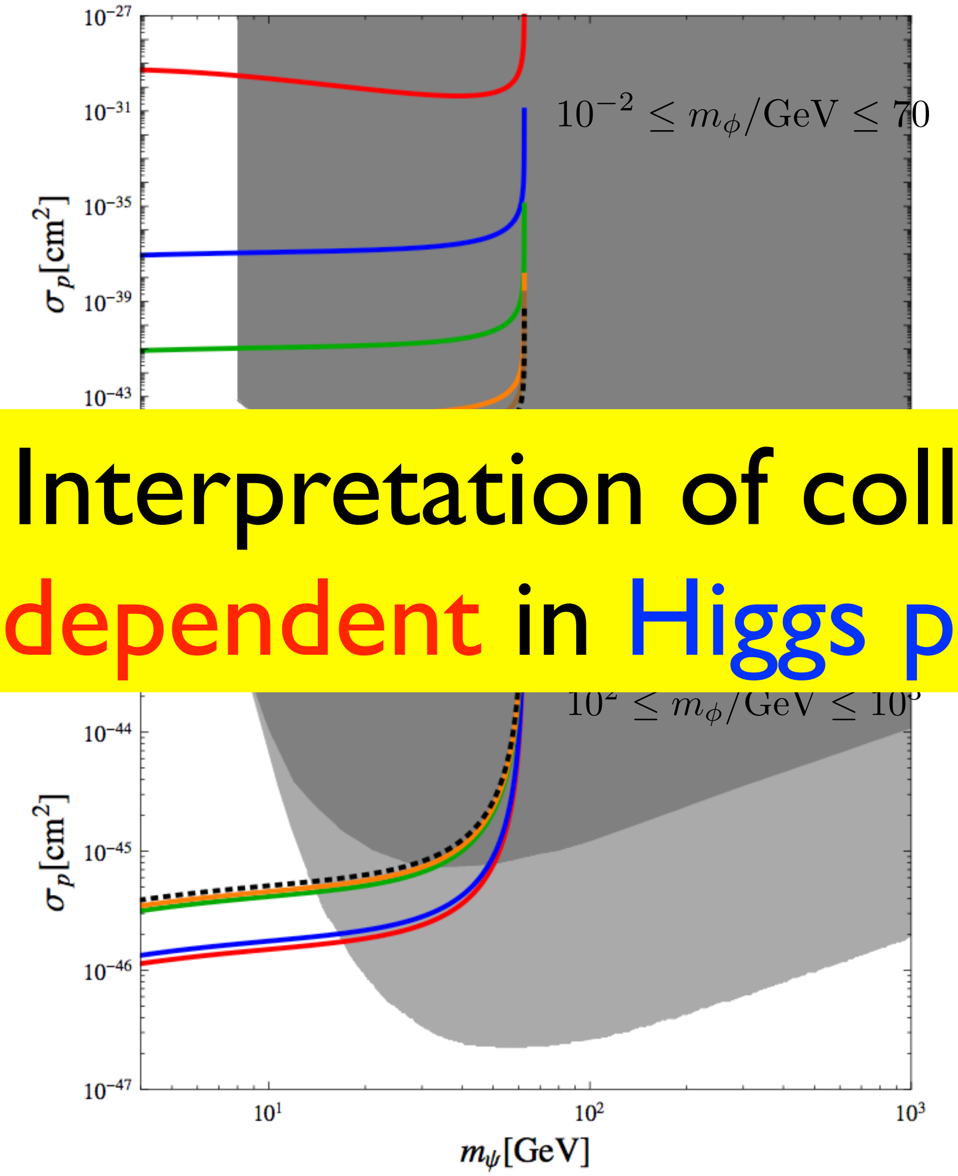

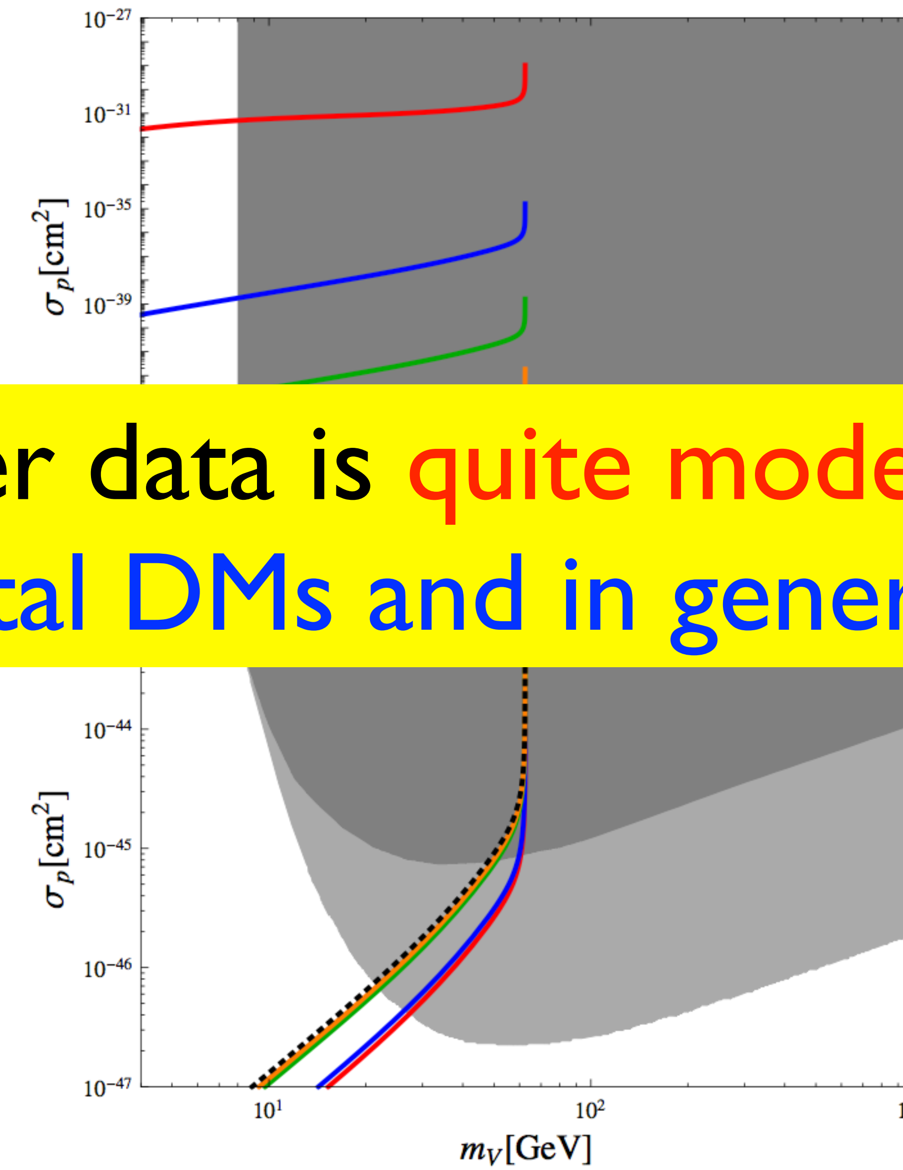

Interpretation of collider data is quite model-dependent in Higgs portal DMs and in general

Invisible H decay into a pair of VDM

[arXiv: 1405.3530, S. Baek, P. Ko & WIPark, PRD]

$$(\Gamma_h^{\rm inv})_{\rm EFT} = \frac{\lambda_{VH}^2}{128\pi}\frac{v_H^2 m_h^3}{m_V^4} \times \left(1 - \frac{4m_V^2}{m_h^2} + 12\frac{m_V^4}{m_h^4}\right)\left(1 - \frac{4m_V^2}{m_h^2}\right)^{1/2} \quad (23)$$

$$m_V \propto g_x Q_\Phi v_\Phi$$

$$\frac{g_X^2}{m_V^2} = \frac{g_X^2}{g_X^2 Q_\Phi^2 v_\Phi^2} \to \frac{1}{v_\Phi^2} = \text{finite}$$

VS.

$$\Gamma_i^{\rm inv} = \frac{g_X^2}{32\pi}\frac{m_i^3}{m_V^2}\left(1 - \frac{4m_V^2}{m_i^2} + 12\frac{m_V^4}{m_i^4}\right)\left(1 - \frac{4m_V^2}{m_i^2}\right)^{1/2}\sin^2\alpha \quad (22)$$

Invisible H decay width : finite for small mV in unitary/renormalizable model

DM searches @ colliders : Beyond the EFT and simplified DM models

- S. Baek, P. Ko, M. Park, WIPark, C. Yu, arXiv:1506.06556, PLB (2016)
- P. Ko and Hiroshi Yokoya, arXiv:1603.04737, JHEP (2016)
- P. Ko, A. Natale, M. Park, H. Yokoya, arXiv:1605.07058, JHEP(2017)
- P. Ko and Jinmian Li, arXiv:1610.03997, PLB (2017)

Why is it broken down in DM EFT ?

The most nontrivial example is the (scalar)x(scalar) operator for DM-N scattering

$$\mathcal{L}_{SS} \equiv \frac{1}{\Lambda_{dd}^2}\bar{q}q\bar{\chi}\chi \quad \text{or} \quad \frac{m_q}{\Lambda_{dd}^3}\bar{q}q\bar{\chi}\chi$$

This operator clearly violates the SM gauge symmetry, and we have to fix this problem

Crossing & WIMP detection

Correct relic density → Efficient annihilation then

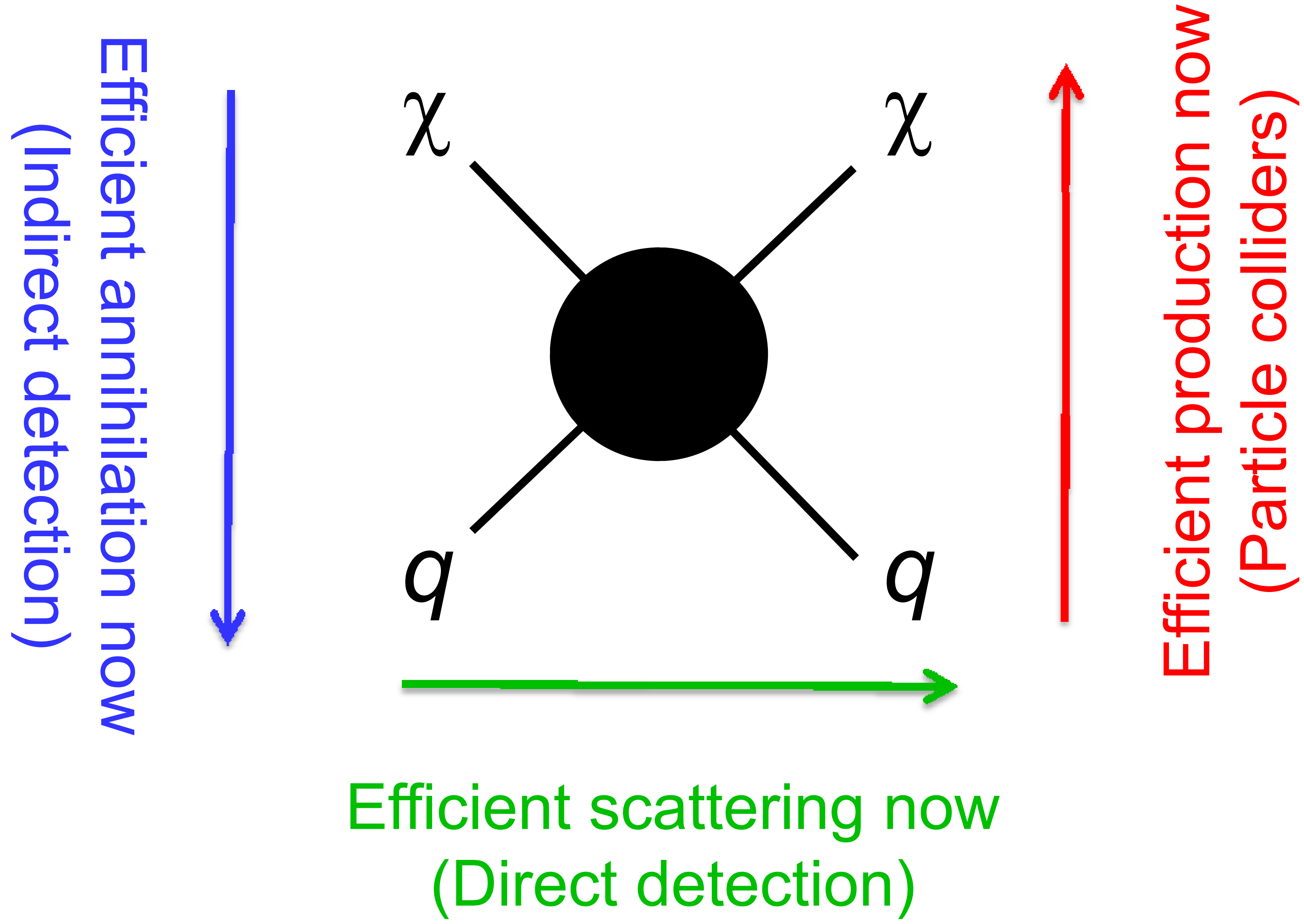

Crossing & WIMP detection

Correct relic density → Efficient annihilation then

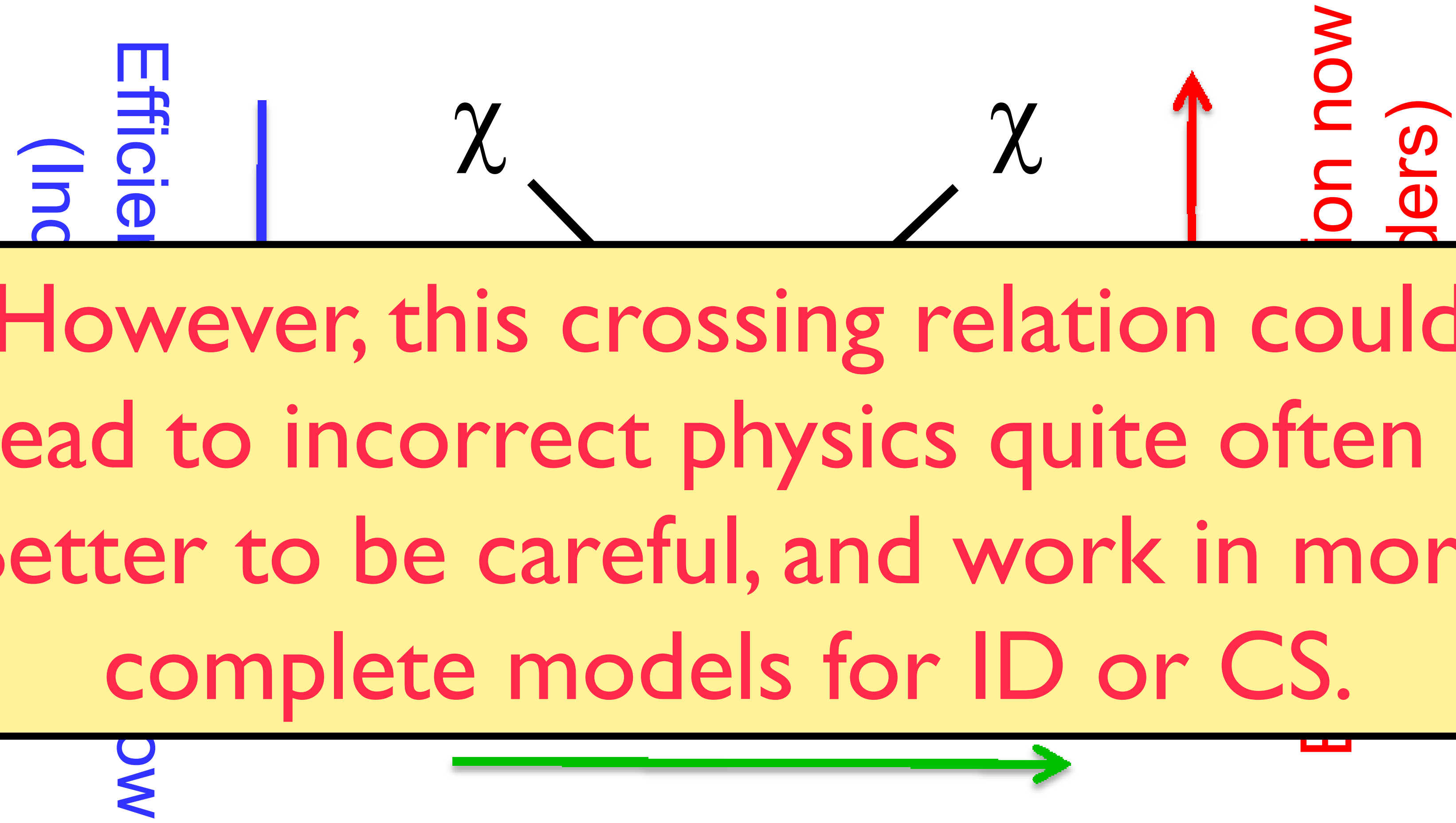

However, this crossing relation could lead to incorrect physics quite often ! Better to be careful, and work in more complete models for ID or CS.

Efficient scattering now
(Direct detection)

Limitation and Proposal

- EFT is good for direct detection, but not for indirect or collider searches as well as thermal relic density calculations in general
- Issues : Violation of Unitarity and SM gauge invariance, Identifying the relevant dynamical fields at energy scale we are interested in, Symmetry stabilizing DM etc.

$$\frac{1}{\Lambda_i^2}\ \bar{q}\Gamma_i q\ \bar{\chi}\Gamma_i\chi \to \frac{g_q g_\chi}{m_\phi^2 - s}\ \bar{q}\Gamma_i q\ \bar{\chi}\Gamma_i\chi$$

- Usually effective operator is replaced by a single propagator in simplified DM models
- This is not good enough, since we have to respect the full SM gauge symmetry (Bell et al for W+missing ET)
- In general we need two propagators, not one propagator, because there are two independent chiral fermions in 4-dim spacetime

arXiv:1605.07058 (with A. Natale, M.Park, H.Yokoya)

for t-channel mediator

Our Model: a 'simplified model' of colored t-channel, spin-0, mediators which produce various mono-x + missing energy signatures (mono-Jet, mono-W, mono-Z, etc.):

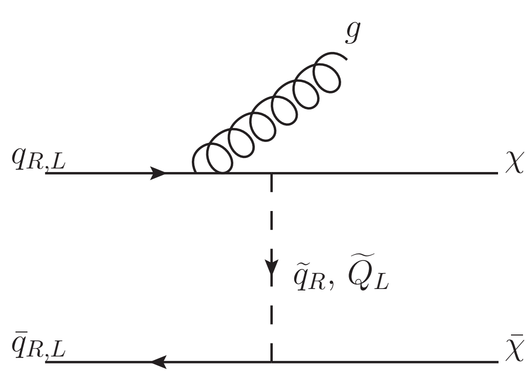

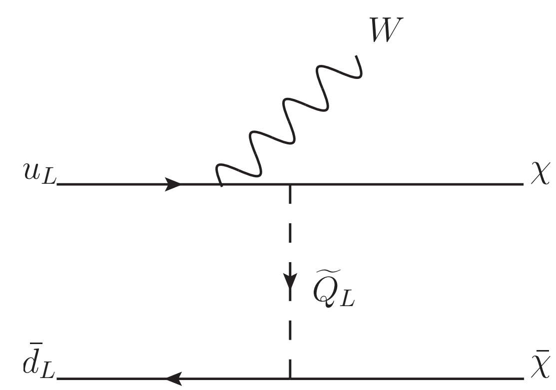

W+missing ET : special

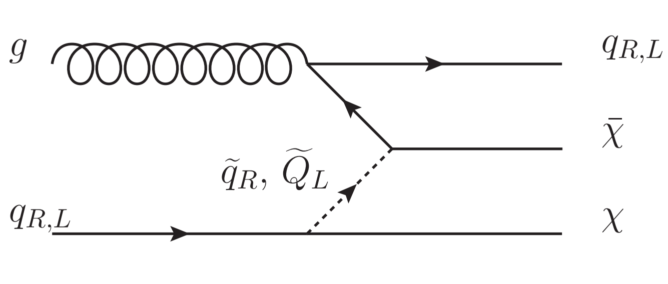

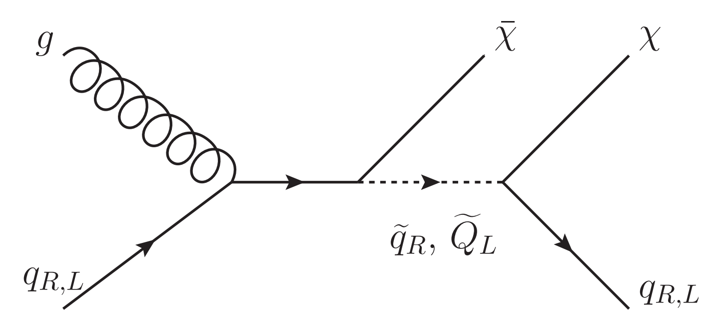

$$\frac{1}{\Lambda_i^2}\ \bar{q}\Gamma_i q\ \bar{\chi}\Gamma_i\chi \to \frac{g_q g_\chi}{m_\phi^2 - s}\ \bar{q}\Gamma_i q\ \bar{\chi}\Gamma_i\chi$$

- This is good only for W+missing ET, and not for other signatures
- The same is also true for (scalar)x(scalar) operator, and lots of confusion on this operator in literature
- Therefore let me concentrate on this case in detail in this talk

$$\overline{Q}_L H d_R \quad \text{or} \quad \overline{Q}_L \widetilde{H} u_R,$$

OK

$$h\bar{\chi}\chi, \qquad s\bar{q}q$$

Both break SM gauge

$$\boxed{\begin{aligned}\mathcal{L} &= \frac{1}{2}m_S^2 S^2 - \lambda_{s\chi} s\bar{\chi}\chi - \lambda_{sq} s\bar{q}q \\ \mathcal{L} &= -\lambda_{h\chi} h\bar{\chi}\chi - \lambda_{hq} h\bar{q}q\end{aligned}}$$

Therefore these Lagragians often used in the literature are not good enough

$$\boxed{s\bar{\chi}\chi \times h\bar{q}q \to \frac{1}{m_s^2}\bar{\chi}\chi\bar{q}q}$$

Need the mixing between s and h

Singlet fermion CDM

Baek, Ko, Park, arXiv:1112.1847

$$
\begin{aligned}
\mathcal{L} \;=\; & \mathcal{L}_{\rm SM} - \mu_{HS} S H^\dagger H - \frac{\lambda_{HS}}{2} S^2 H^\dagger H \\
& + \frac{1}{2}(\partial_\mu S \partial^\mu S - m_S^2 S^2) - \mu_S^3 S - \frac{\mu_S'}{3} S^3 - \frac{\lambda_S}{4} S^4 \\
& + \overline{\psi}(i \not{\partial} - m_{\psi_0})\psi - \lambda S \overline{\psi}\psi
\end{aligned}
$$

mixing

invisible decay

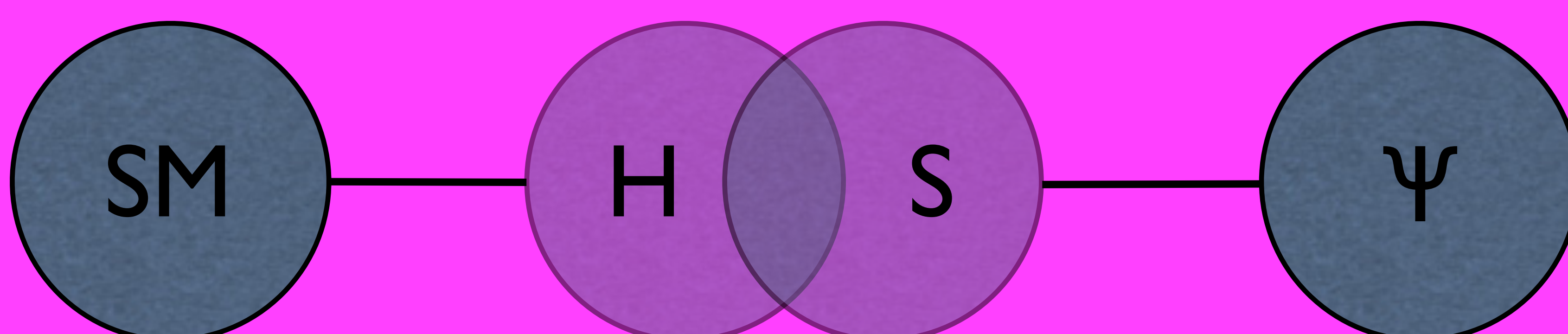

Production and decay rates are suppressed relative to SM.

This simple model has not been studied properly !!

Full Theory Calculation

$$\boxed{\chi(p) + q(k) \to \chi(p') + q(k')}$$

$$\begin{aligned}
\mathcal{M} &= \overline{u(p')}u(p)\overline{u(q')}u(q)\ \frac{m_q}{v}\lambda_s \sin\alpha\cos\alpha\ \left[\frac{1}{t - m_{125}^2 + i m_{125}\Gamma_{125}} - \frac{1}{t - m_2^2 + i m_s \Gamma_2}\right] \\
&\to \overline{u(p')}u(p)\overline{u(q')}u(q)\ \frac{m_q}{2v}\lambda_s \sin 2\alpha \left[\frac{1}{m_{125}^2} - \frac{1}{m_2^2}\right] \\
&\to \overline{u(p')}u(p)\overline{u(q')}u(q)\ \frac{m_q}{2v}\lambda_s \sin 2\alpha \frac{1}{m_{125}^2} \equiv \frac{m_q}{\Lambda_{dd}^3}\overline{u(p')}u(p)\overline{u(q')}u(q)
\end{aligned}$$

$$\begin{aligned}
\Lambda_{dd}^3 &\equiv \frac{2m_{125}^2 v}{\lambda_s \sin 2\alpha}\left(1 - \frac{m_{125}^2}{m_2^2}\right)^{-1} \\
\bar{\Lambda}_{dd}^3 &\equiv \frac{2m_{125}^2 v}{\lambda_s \sin 2\alpha}
\end{aligned}$$

Monojet+missing ET

Can be obtained by crossing : s <>t

$$\frac{1}{\Lambda_{dd}^3} \rightarrow \frac{1}{\Lambda_{dd}^3}\left[\frac{m_{125}^2}{s-m_{125}^2+im_{125}\Gamma_{125}} - \frac{m_{125}^2}{s-m_2^2+im_2\Gamma_2}\right] \equiv \frac{1}{\Lambda_{col}^3(s)}$$

There is no single scale you can define
for collider search for missing ET

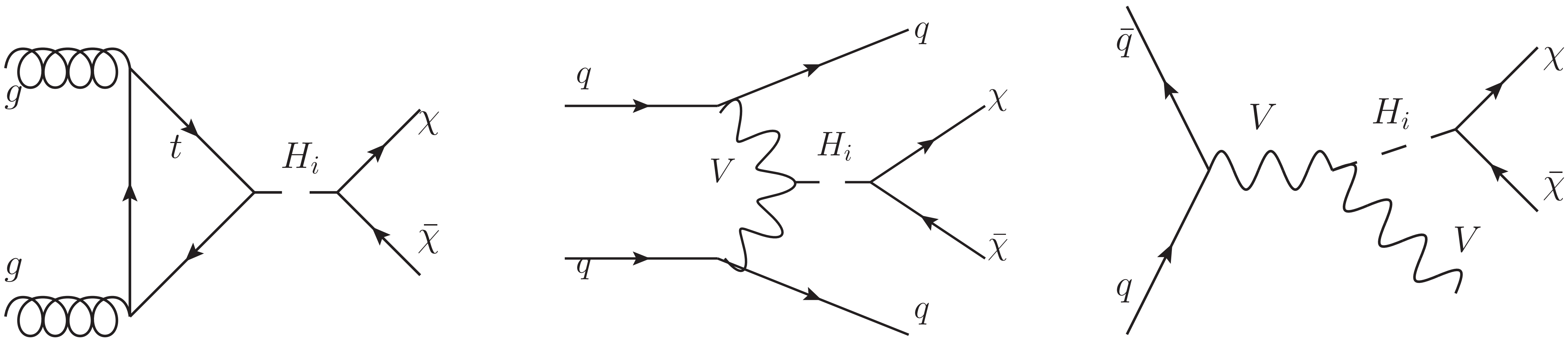

Figure 1: The dominant DM production processes at LHC.

Interference between 2 scalar bosons could be important in certain parameter regions

$$\frac{d\sigma_i}{dm_{\chi\chi}} \propto \left| \frac{\sin 2\alpha \; g_\chi}{m_{\chi\chi}^2 - m_{H_1}^2 + i m_{H_1}\Gamma_{H_1}} - \frac{\sin 2\alpha \; g_\chi}{m_{\chi\chi}^2 - m_{H_2}^2 + i m_{H_2}\Gamma_{H_2}} \right|^2$$

$$\boxed{\sin\alpha = 0.2, g_\chi = 1, m_\chi = 80\mathrm{GeV}}$$

Interference effects

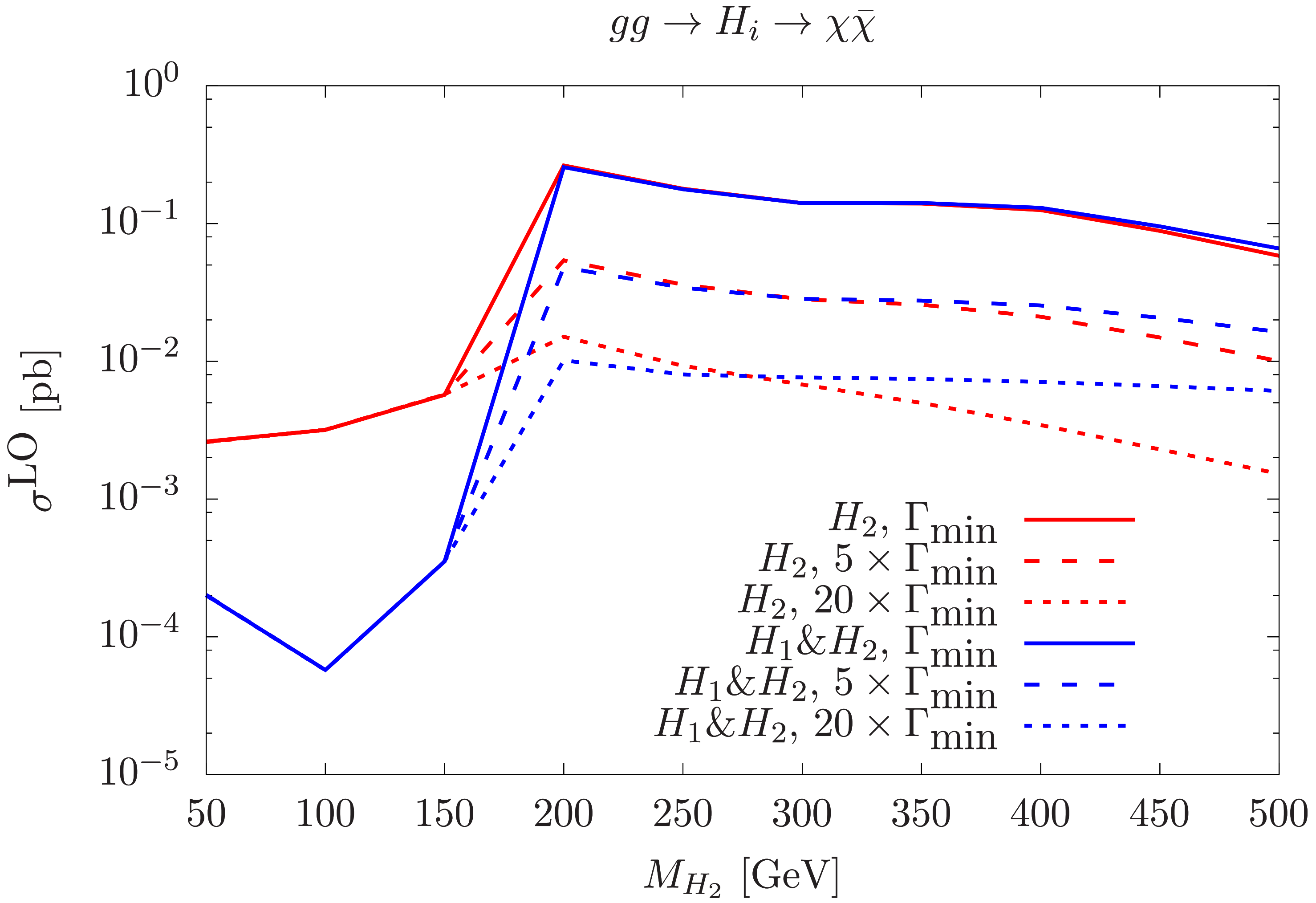

Figure 2: The LO cross section for gluon-gluon fusion process at 13 TeV LHC. The meanings of the different line types are explained in the text and the similar strategy will be used in all figures.

Parton level distributions

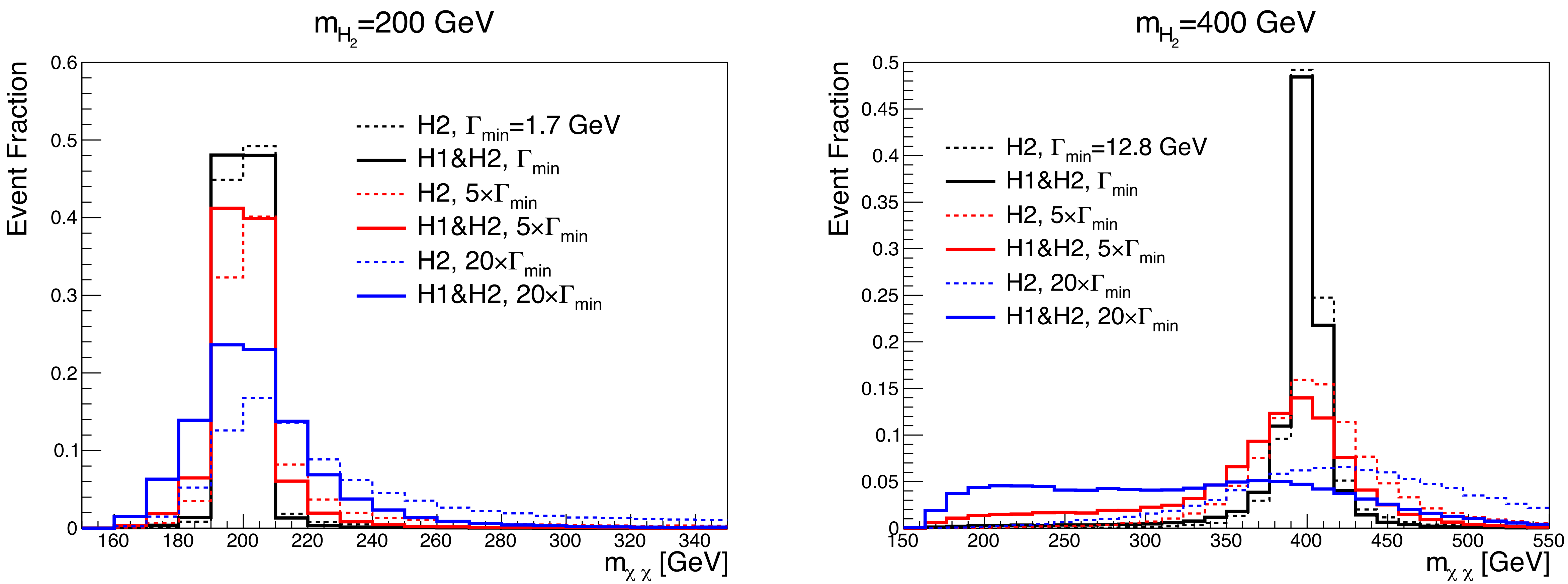

Figure 3: The parton level distributions of $m_{\chi\bar{\chi}}$ for gluon-gluon fusion process at 13 TeV LHC.

Exclusion limits with interference effects

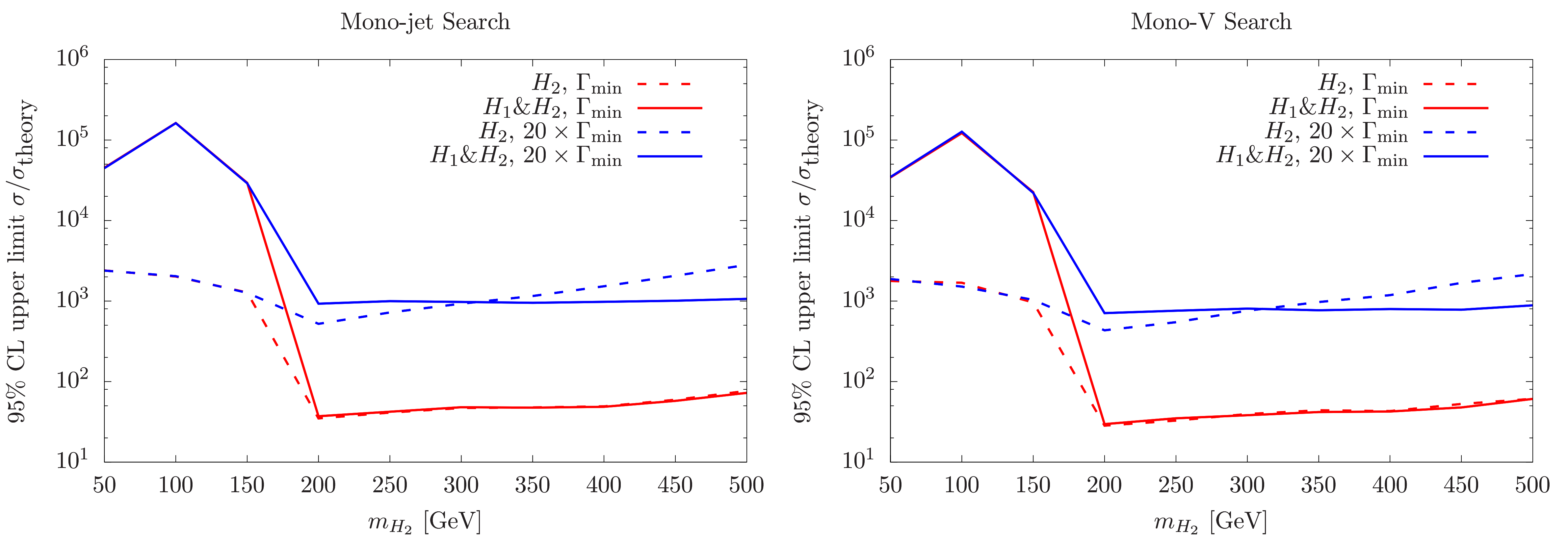

Figure 8: The CMS exclusion limits on our simplified models. Left: upper limit from mono-jet search. Right: upper limit from mono-V search.

- P. Ko and Jinmian Li, 1610.03997, PLB (2017)
- S. Baek, P. Ko and Jinmian Li, 1701.04131

- EFT : Effective operator $\mathcal{L}_{int} = \frac{m_q}{\Lambda_{dd}^3}\bar{q}q\bar{\chi}\chi$
- S.M.: Simple scalar mediator S of
  $\mathcal{L}_{int} = \left(\frac{m_q}{v_H}\sin\alpha\right) S\bar{q}q - \lambda_s \cos\alpha S\bar{\chi}\chi$
- H.M.: A case where a Higgs is a mediator
  $\mathcal{L}_{int} = -\left(\frac{m_q}{v_H}\cos\alpha\right) H\bar{q}q - \lambda_s \sin\alpha H\bar{\chi}\chi$
- H.P.: Higgs portal model as in eq. (2).

$$\text{H.P.} \xrightarrow[m_{H_2}^2 \gg \hat{s}]{} \text{H.M.},$$
$$\text{S.M.} \xrightarrow[m_S^2 \gg \hat{s}]{} \text{EFT},$$
$$\text{H.M.} \neq \text{EFT}\,.$$

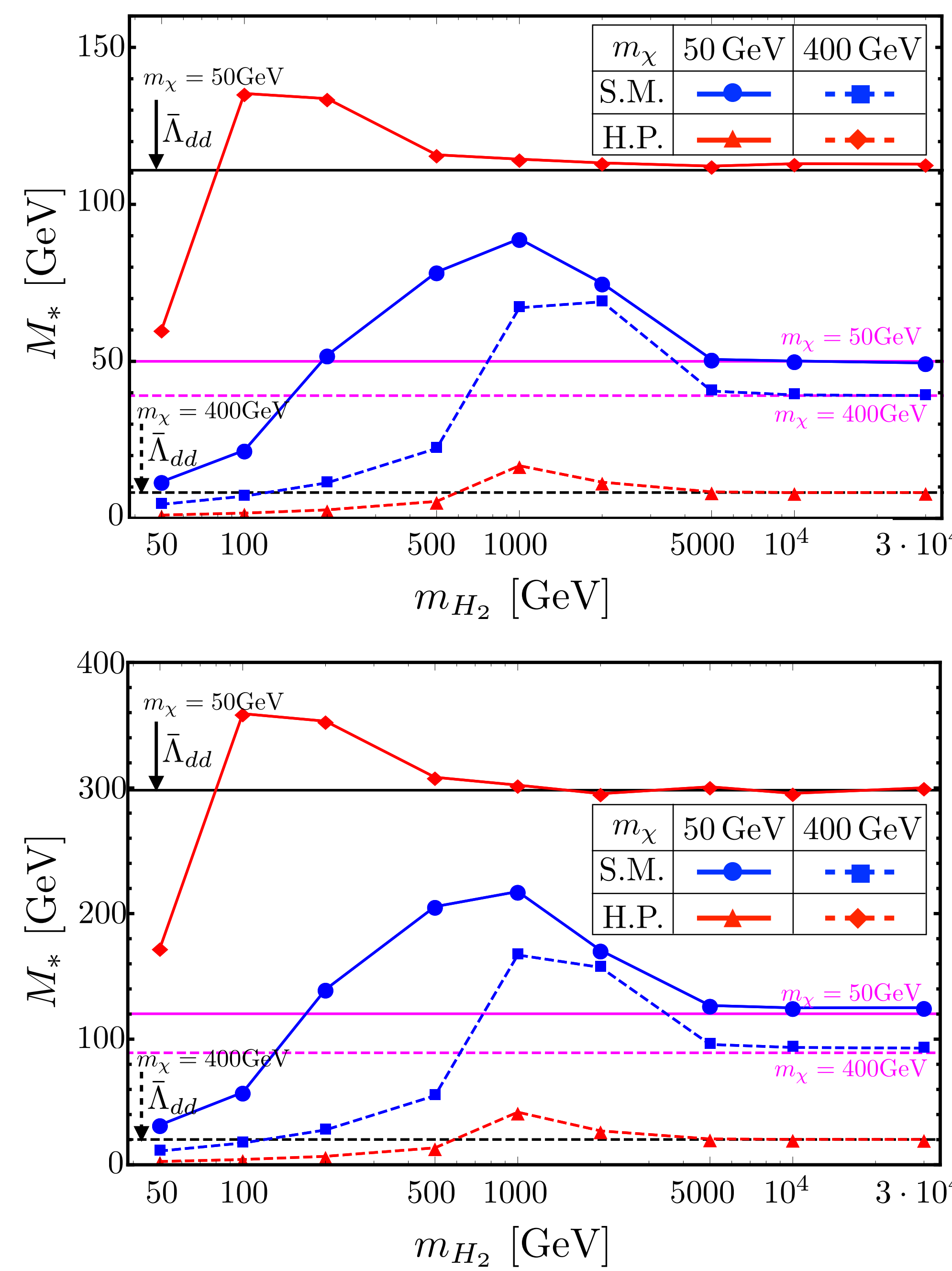

FIG. 3: The experimental bounds on M_* at 90% C.L. as a function of m_{H_2} (m_S in S.M. case) in the monojet+$\not{E}_T$ search (upper) and $t\bar{t} + \not{E}_T$ search (lower). Each line corresponds to the EFT approach (magenta), S.M. (blue), H.M. (black), and H.P. (red), respectively. The bound of S.M., H.M., and H.P., are expressed in terms of the effective mass M_* through the Eq.(16)-(20). The solid and dashed lines correspond to $m_\chi = 50$ GeV and 400 GeV in each model, respectively.

A General Comment

assume: $2m_\chi \ll m_{125} \ll m_2 \ll \sqrt{s}$

$$\begin{aligned}
\sigma(\sqrt{s}) &= \int_0^1 d\tau \sum_{a,b} \frac{d\mathcal{L}_{ab}}{d\tau} \hat{\sigma}(\hat{s} \equiv \tau s) \\
&= \left[\int_{4m_\chi^2/s}^{m_{125}^2/s} d\tau + \int_{m_{125}^2/s}^{m_2^2/s} d\tau + \int_{m_2^2/s}^{1} d\tau \right] \sum_{a,b} \frac{d\mathcal{L}_{ab}}{d\tau} \hat{\sigma}(\hat{s} \equiv \tau s)
\end{aligned}$$

For each integration region for tau, we have to use different EFT

No single EFT applicable to the entire tau regions

Indirect Detection

$$
\begin{aligned}
|\frac{1}{\Lambda_{ann}^3}| &\simeq \frac{1}{\Lambda_{dd}^3}\left|\frac{m_{125}^2}{4m_\chi^2 - m_{125}^2 + im_{125}\Gamma_{125}} - \frac{m_{125}^2}{4m_\chi^2 - m_2^2 + im_2\Gamma_2}\right| \\
&\to \frac{1}{\Lambda_{dd}^3}\left|\frac{m_{125}^2}{4m_\chi^2 - m_{125}^2 + im_{125}\Gamma_{125}}\right| \neq \frac{1}{\Lambda_{dd}^3}
\end{aligned}
$$

- Again, no definite correlations between two scales in DD and ID
- Also one has to include other channels depending on the DM mass

Pseudoscalar Mediator with Higgs portal

S. Baek, P. Ko, Jinmian Li, arXiv:1701.04131
to appear in PRD

Pseudoscalar portal DM

(S. Baek, P. Ko, Jinmian Li, arXiv:1701.04131)

$$\frac{1}{\Lambda^2}\bar{f}f\bar{\chi}\gamma_5\chi$$

- Highly suppressed for SI/SD x-section
- DM pair annihilation in the S-wave

Its simplest UV completion:
(different from 2HDM portal)

$$\begin{aligned}\mathcal{L} = & \bar{\chi}(i\partial\cdot\gamma - m_\chi - ig_\chi a\gamma^5)\chi + \frac{1}{2}\partial_\mu a\partial^\mu a - \frac{1}{2}m_a^2 a^2 \\ & -(\mu_a a + \lambda_{Ha}a^2)\left(H^\dagger H - \frac{v_h^2}{2}\right) - \frac{\mu_a'}{3!}a^3 - \frac{\lambda_a}{4!}a^4 \\ & -\lambda_H\left(H^\dagger H - \frac{v_h^2}{2}\right)^2 \quad . \end{aligned} \qquad (1)$$

see also Karim Ghorbani, arXiv:1408.4929 [hep-ph]

Interaction Lagrangians

$$\mathcal{L}_{\rm int} = -ig_\chi(H_0 \sin\alpha + A\cos\alpha)\ \bar\chi\gamma^5\chi - (H_0\cos\alpha - A\sin\alpha) \times \left[\sum_f \frac{m_f}{v_h}\bar f f - \frac{2m_W^2}{v_h}W_\mu^+W^{-\mu} - \frac{m_Z^2}{v_h}Z_\mu Z^\mu\right] \quad (7)$$

For comparison, let us define 2 other cases

$$\mathcal{L}_{\rm int}^{\rm SS} = -g_\chi(H_1 \sin\alpha + H_2\cos\alpha)\ \bar\chi\chi - (H_1\cos\alpha - H_2\sin\alpha) \times \left[\sum_f \frac{m_f}{v_h}\bar f f - \frac{2m_W^2}{v_h}W_\mu^+W^{-\mu} - \frac{m_Z^2}{v_h}Z_\mu Z^\mu\right] \quad (12)$$

(Higgs portal)

$$\mathcal{L}_{\rm int}^{\rm AA} = -ig_\chi(a \sin\alpha + A\cos\alpha)\ \bar\chi\gamma^5\chi - i(a\cos\alpha - A\sin\alpha)\sum_f \frac{m_f}{v_h}\bar f\gamma^5 f \quad (13)$$

(2HDM+a portal)

DM phenomenology

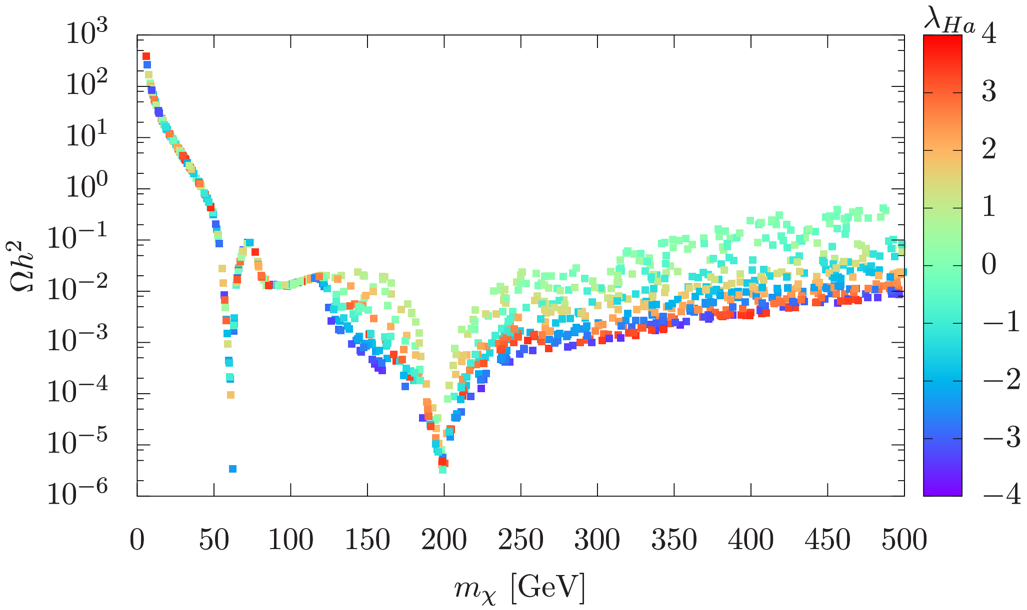

FIG. 1. Relic density with varying DM mass, for $m_A = 400$ GeV, $g_\chi = 1$ and $\alpha = 0.3$. Color code indicates the value of λ_{Ha}.

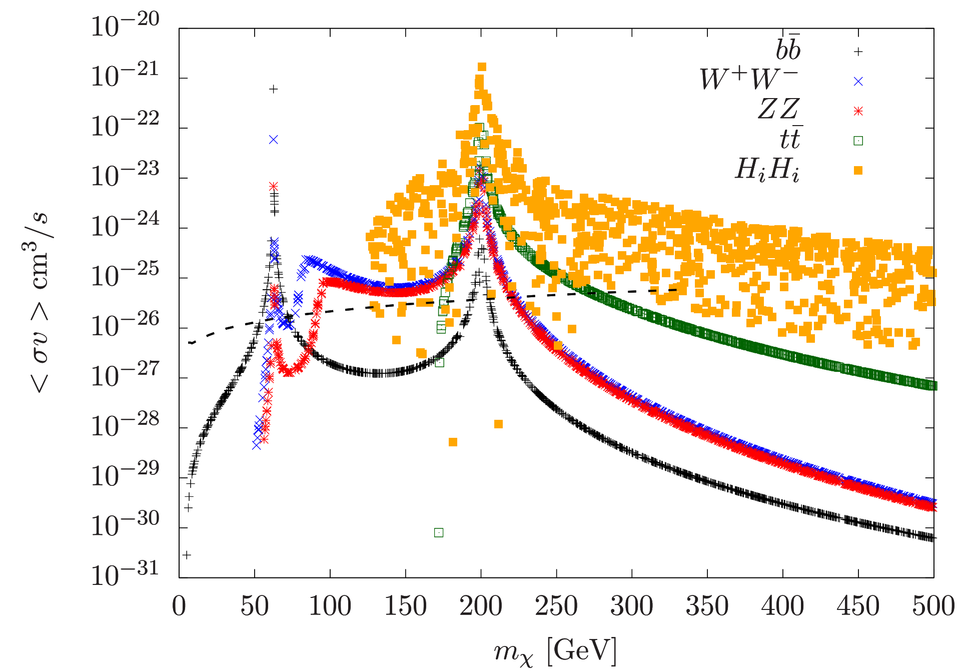

FIG. 2. The cross sections for different DM annihilation (at rest) channels. The dashed black curve correspond to the 95% CL exclusion limit on $b\bar{b}$ channel obtained from Milky Way Dwarf Spheroidal Galaxies with Six Years of Fermi-LAT Data [55].

Good scenario for DM phenomenology in terms of (in)direct detection expt's

Collider Searches

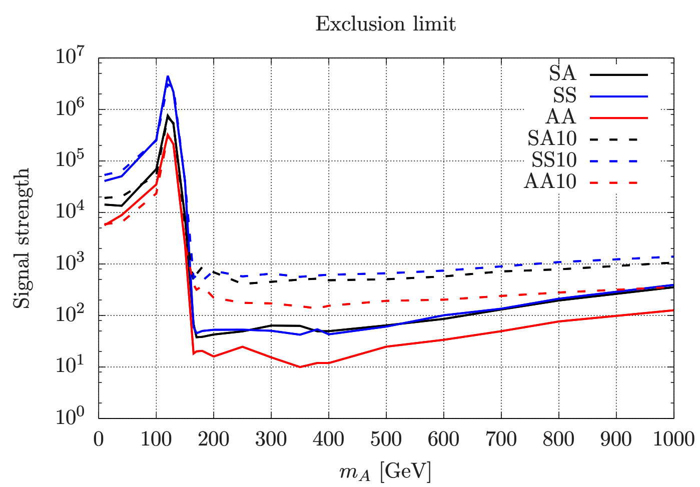

FIG. 5. The 95% CL exclusion limits from the ATLAS mono-jet search at 13 TeV with integrated luminosity of 3.2 fb^{-1} . The dashed curves correspond to models with ten times larger total width of A than $\Gamma_{\min}$ due to the opening of new decay channels.

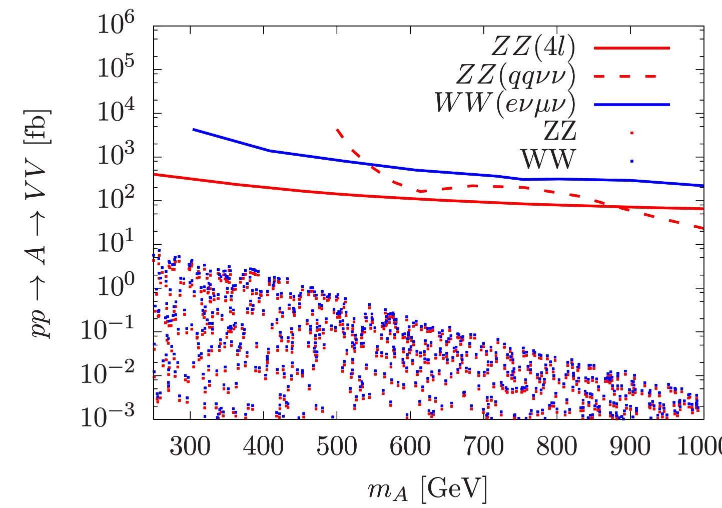

FIG. 6. Bounds correspond to the LHC searches for two vector boson resonance. The production cross sections of ZZ (WW) at 13 TeV in our model are shown by red (blue) points.

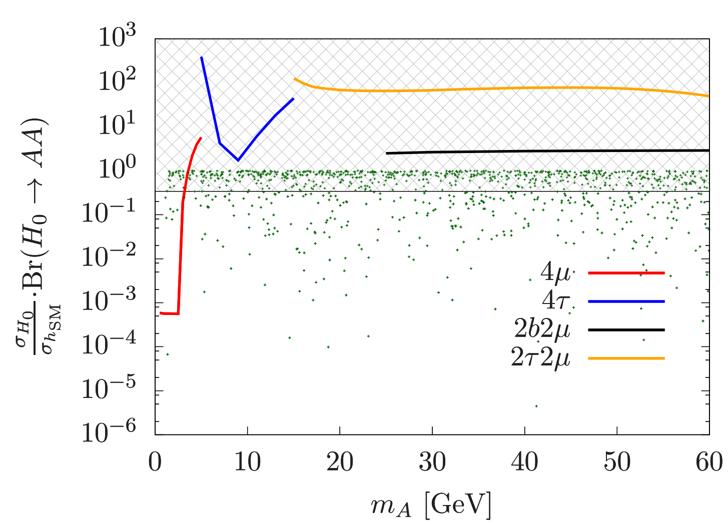

FIG. 7. Bounds correspond to the LHC searches for light boson pair from the SM Higgs decay. The shaded region is excluded by the Higgs precision measurement. Our models are shown by dark green points.

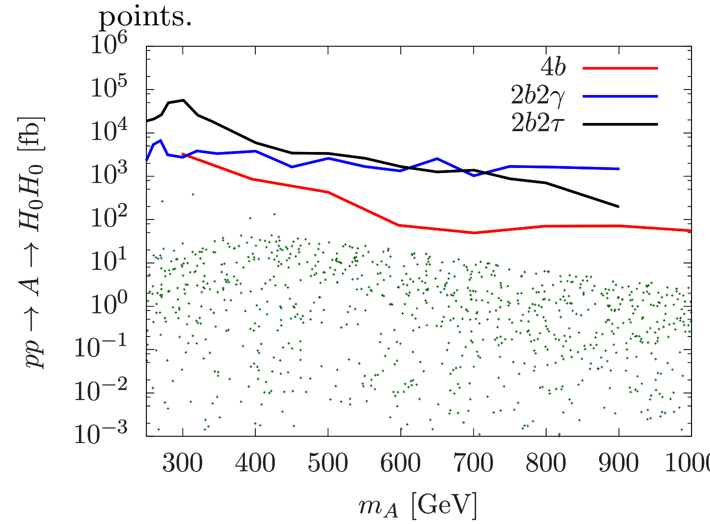

FIG. 8. Bounds correspond to the LHC di-Higgs searches in different final states. The production cross section of our models at 13 TeV are shown by dark green points.

DM Searches @ ILC 500

arXiv:1603.04737, 2/ H. Yokoya, JHEP
arXiv:1705.02149, w/ T. Kamon, J. Li, EPJC

Interaction Lagrangians

Scalar DM

$$\mathcal{L}_{\rm SDM}^{\rm int} = -h \left(\frac{2m_W^2}{v_h} W_\mu^+ W^{-\mu} + \frac{m_Z^2}{v_h} Z_\mu Z^\mu \right) - \lambda_{HS} v_h \, h S^2 .$$

Singlet FDM

$$\mathcal{L}_{\rm FDM}^{\rm int} = - \left(H_1 \cos\alpha + H_2 \sin\alpha \right) \left(\sum_f \frac{m_f}{v_h} \bar{f} f - \frac{2m_W^2}{v_h} W_\mu^+ W^{-\mu} - \frac{m_Z^2}{v_h} Z_\mu Z^\mu \right) + g_\chi \left(H_1 \sin\alpha - H_2 \cos\alpha \right) \, \bar{\chi}\chi \; .$$

Vector DM

$$\mathcal{L}_{\rm VDM}^{\rm int} = - \left(H_1 \cos\alpha + H_2 \sin\alpha \right) \left(\sum_f \frac{m_f}{v_h} \bar{f} f - \frac{2m_W^2}{v_h} W_\mu^+ W^{-\mu} - \frac{m_Z^2}{v_h} Z_\mu Z^\mu \right) - \frac{1}{2} g_V m_V \left(H_1 \sin\alpha - H_2 \cos\alpha \right) \, V_\mu V^\mu \; .$$

NB: One can not ignore 125 GeV Higgs by hand:
Not Well defined EFT, Breaks gauge invariance, etc.

General Features

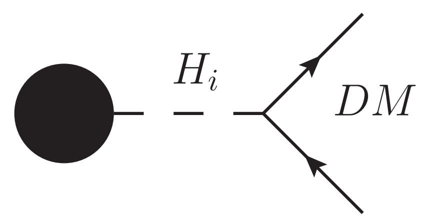

, $\qquad t \equiv m_{DD}^2$

$$\frac{d\sigma_{\rm SDM}}{dt} \propto \sigma^{h*}_{\rm SDM} \times |\frac{1}{t - m_h^2 + i m_h \Gamma_h}|^2,$$

$$\frac{d\sigma_{\rm FDM}}{dt} \propto \sigma^{h*}_{\rm FDM} \times |\frac{1}{t - m_{H_1}^2 + i m_{H_1}\Gamma_{H_1}} - \frac{1}{t - m_{H_2}^2 + i m_{H_2}\Gamma_{H_2}}|^2 \cdot \left(2t - 8m_\chi^2\right),$$

$$\frac{d\sigma_{\rm VDM}}{dt} \propto \sigma^{h*}_{\rm VDM} \times |\frac{1}{t - m_{H_1}^2 + i m_{H_1}\Gamma_{H_1}} - \frac{1}{t - m_{H_2}^2 + i m_{H_2}\Gamma_{H_2}}|^2 \cdot \left(2 + \frac{(t - 2m_D^2)^2}{4m_V^4}\right).$$

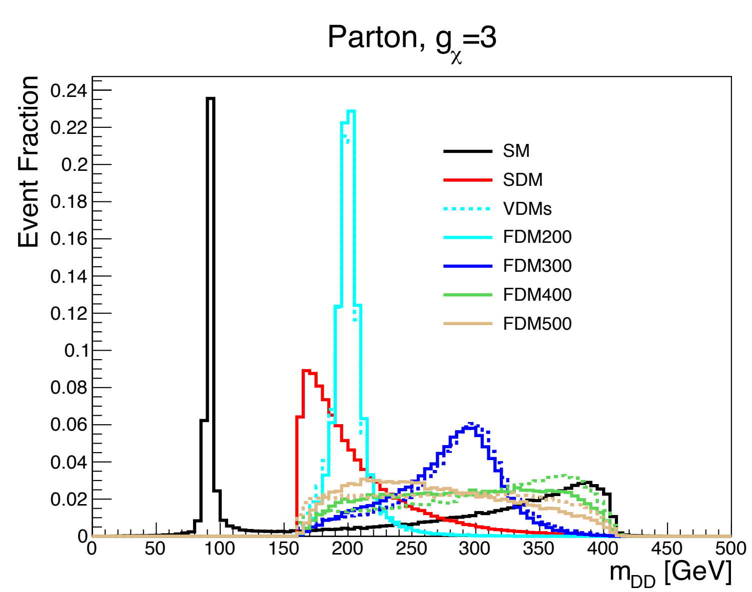

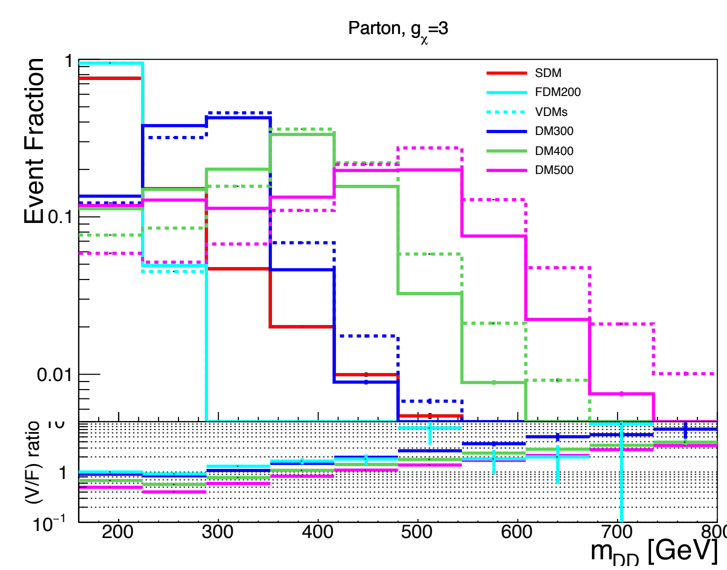

Fix DM mass = 80 GeV, sing(alpha) = 0.3, and vary H2 mass (200,300,400,500) GeV

Asymtotic behavior in the full theory

$$\text{ScalarDM}: \quad G(t) \sim \frac{1}{(t-m_H^2)^2 + m_H^2\Gamma_H^2} \tag{5.7}$$

$$\text{SFDM}: \quad G(t) \sim \left| \frac{1}{t-m_1^2+im_1\Gamma_1} - \frac{1}{t-m_2^2+im_2\Gamma_2} \right|^2 \left(t-4m_\chi^2\right) \tag{5.8}$$

$$\to |\frac{1}{t^2}|^2 \times t \sim \frac{1}{t^3} \ (\text{as } t \to \infty) \tag{5.9}$$

$$\text{VDM}: \quad G(t) \sim \left| \frac{1}{t-m_1^2+im_1\Gamma_1} - \frac{1}{t-m_2^2+im_2\Gamma_2} \right|^2 \left[2 + \frac{(t-2m_V^2)^2}{4m_V^4}\right] \tag{5.10}$$

$$\to |\frac{1}{t^2}|^2 \times t^2 \sim \frac{1}{t^2} \ (\text{as } t \to \infty) \tag{5.11}$$

Asymptotic behavior w/o the 2nd Higgs (EFT)

$$\text{SFDM}: \quad G(t) \sim \frac{1}{(t-m_H^2)^2 + m_H^2\Gamma_H^2} \left(t-4m_\chi^2\right)$$

$$\to \frac{1}{t} \ (\text{as } t \to \infty)$$

$$\text{VDM}: \quad G(t) \sim \frac{1}{(t-m_H^2)^2 + m_H^2\Gamma_H^2} \left[2 + \frac{(t-2m_V^2)^2}{4m_V^4}\right]$$

$$\to \text{constant} \ (\text{as } t \to \infty)$$

Unitarity violated !

DM productions @ ILC

The dominant DM production process:

$$e^+e^- \to Z(\to ff)\ H_{1,2}^{(*)}(\to DD)$$

DM pair four-momentum:

$$P^\mu_{DD} = P^\mu_{e^+} + P^\mu_{e^-} - P^\mu_Z = (\sqrt{s} - E_Z, -\vec{p}_Z)$$

DM pair invariant mass:

$$m^2_{DD} = s + m^2_Z - 2E_Z\sqrt{s}$$

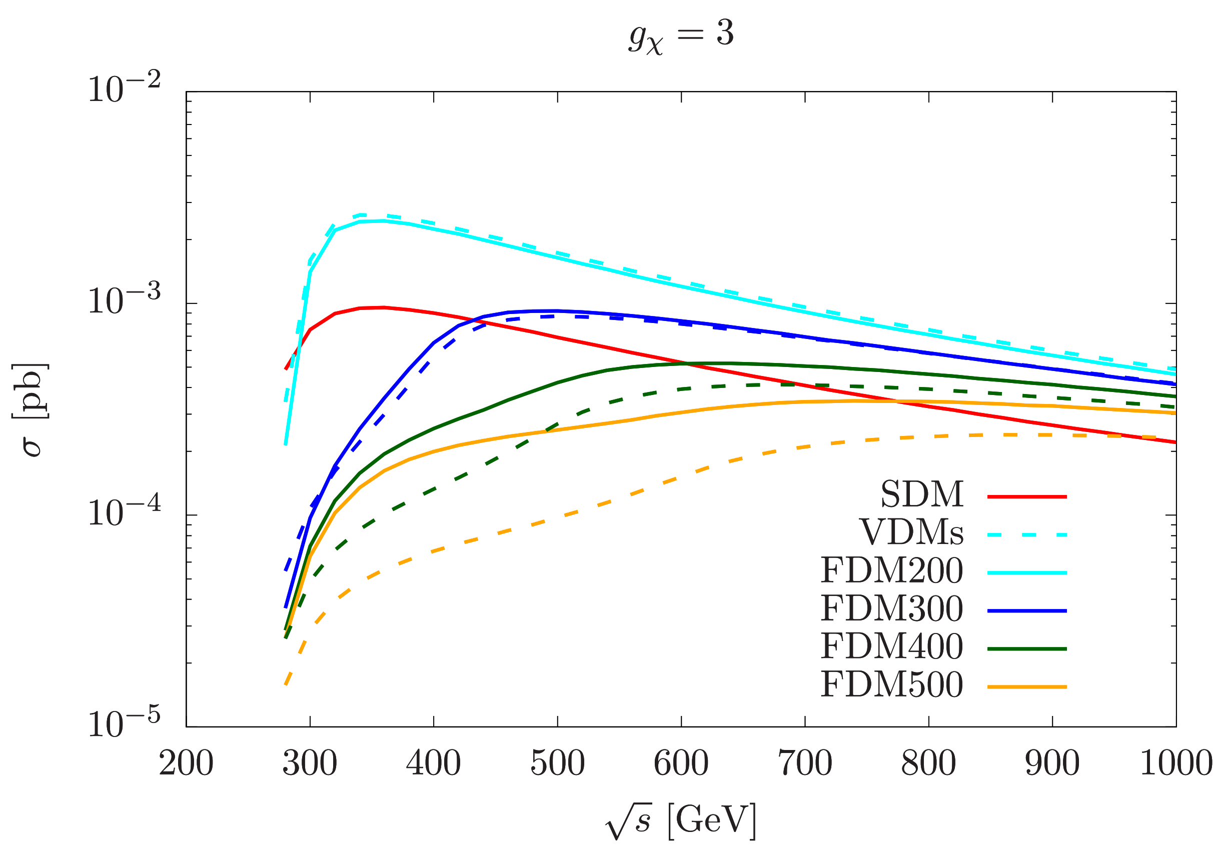

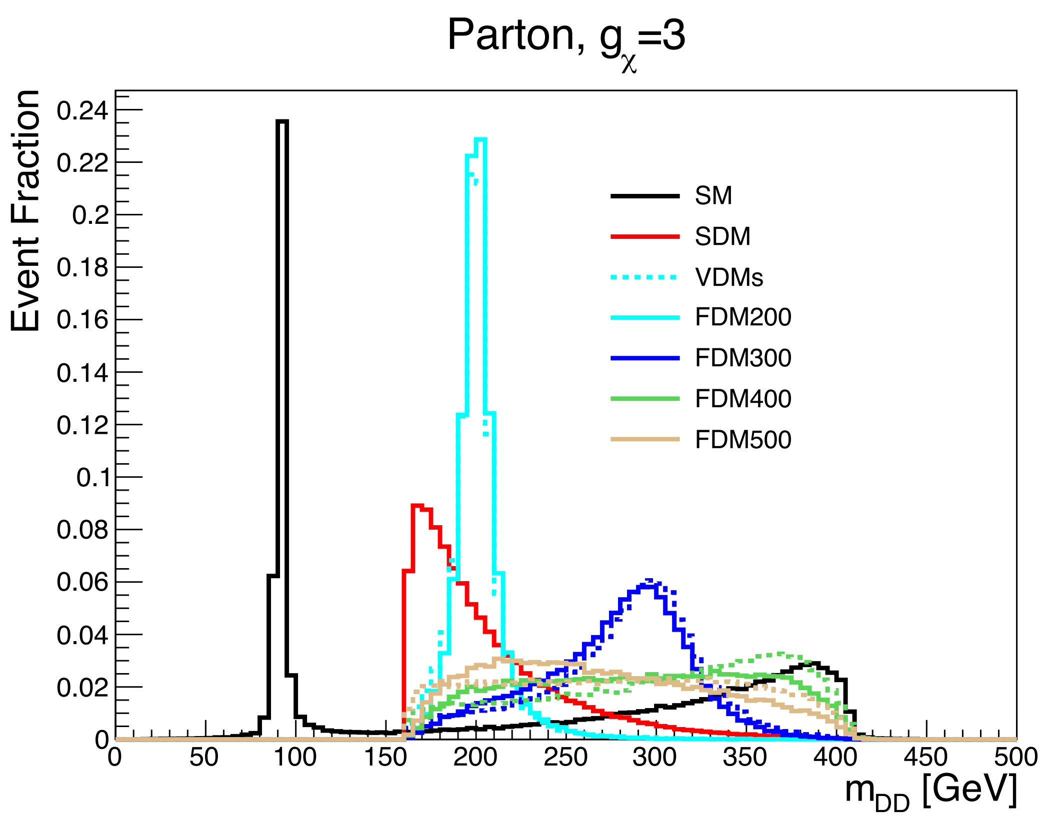

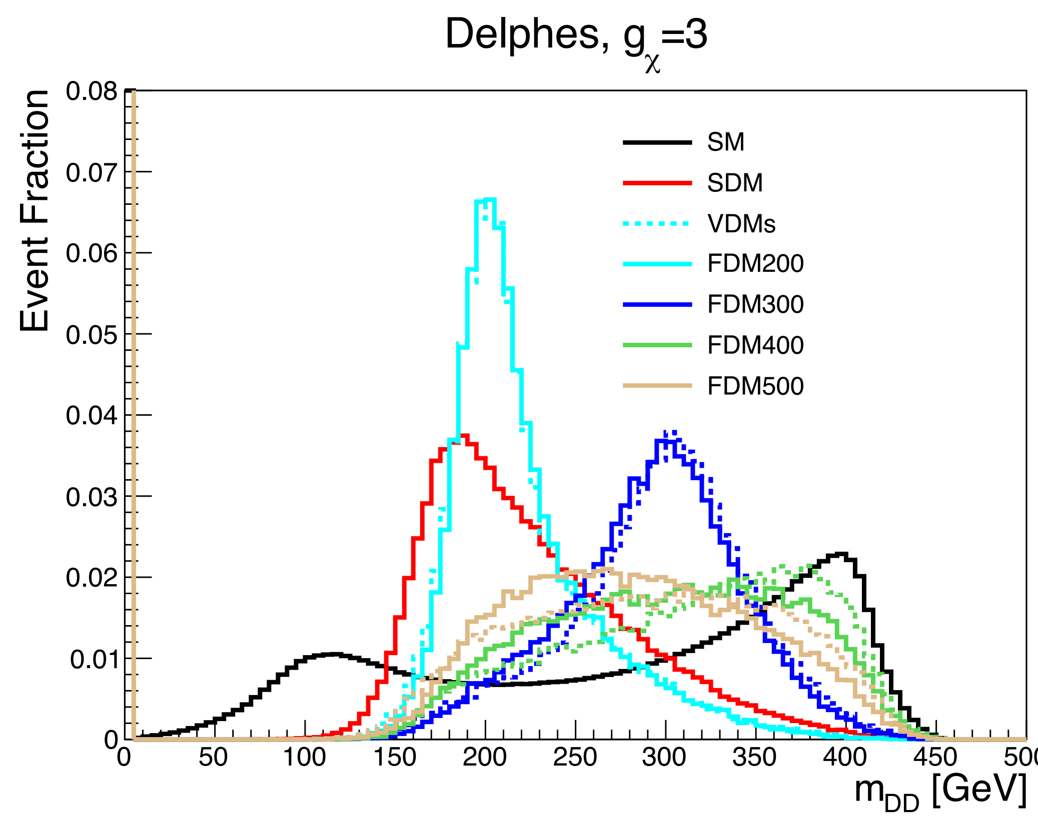

Dominant background processes:

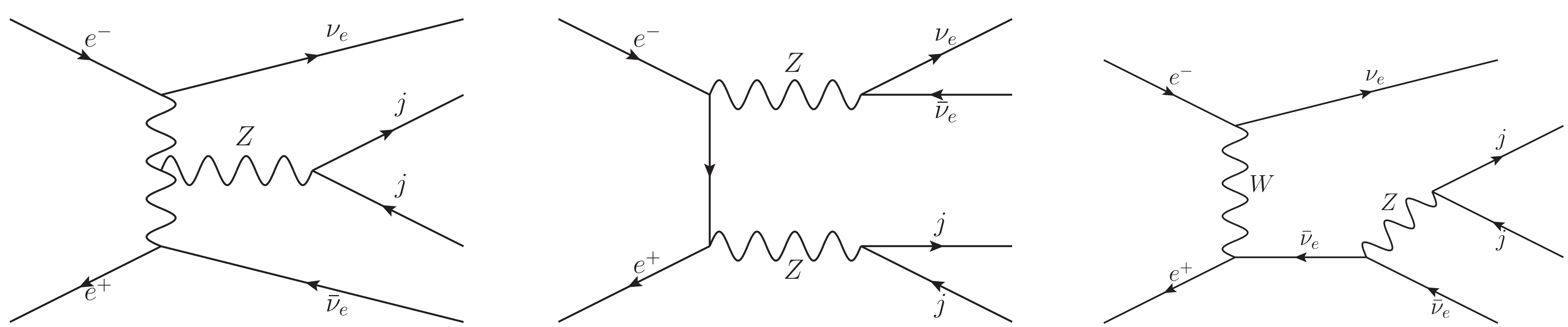

Discovery prospects of hadronic channels (SFDM)

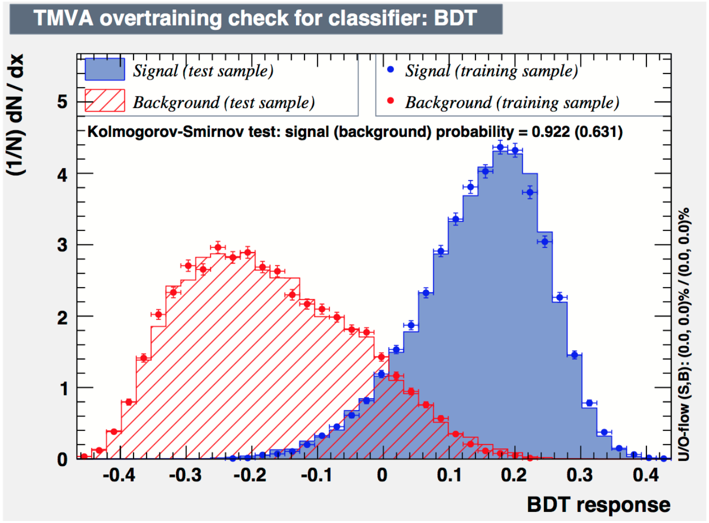

Preselection cuts:

- Lepton veto
- Exactly two jets
- $E_T^{\text{miss}} > 50$ GeV

Boosted decision tree analysis with inputs:

$$m_{DD},\ p_T(j_1),\ p_T(Z),\ E_T^{\text{miss}},\ \Delta\phi^{\text{min}},\ p_T(j_2),\ m_{jj}$$

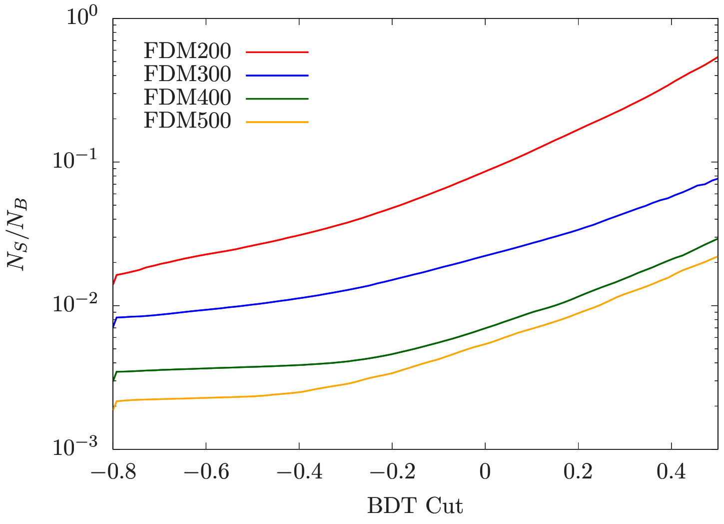

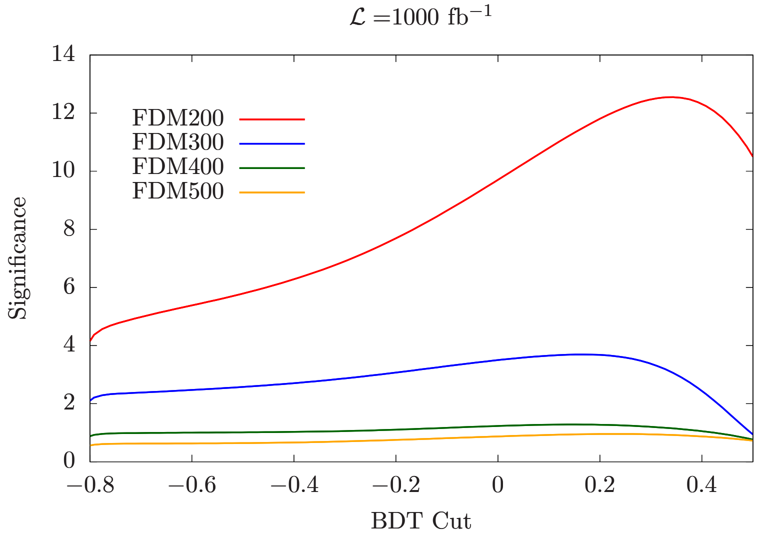

Discovery prospects of hadronic channels (SFDM)

	FDM200	FDM300	FDM400	FDM500
σ^0 [fb]	1.643	0.9214	0.4221	0.2526
ϵ^{pre}	0.796	0.717	0.655	0.698
BDT	0.3615	0.2132	0.1929	0.2129
$N_S/1000\ \text{fb}^{-1}$	697.8	410.5	148	102
$N_B/1000\ \text{fb}^{-1}$	2248.5	11453.5	12736	10898
$N_S/\sqrt{N_S+N_B}$	12.85	3.769	1.31	0.97

Searches @100 TeV pp

arXiv: 1712.05123, EPJC (2018)
w/ B. Dutta, T. Kamon, J. Li

Signal : Monojet ?

M. R Buckley et.al.;

U. Haisch et.al.;

F.Boudjema et.al.;

J. Ellis et.al. ...

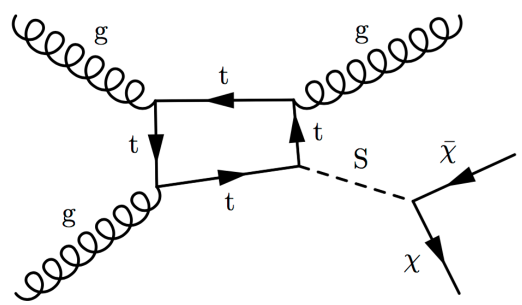

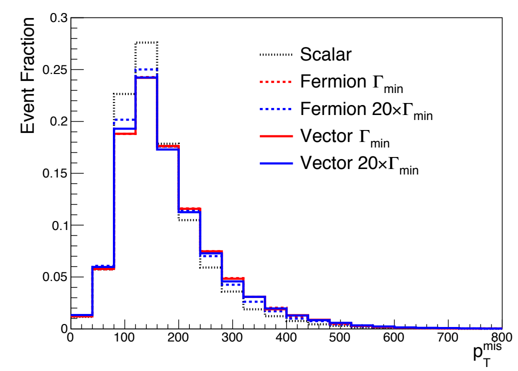

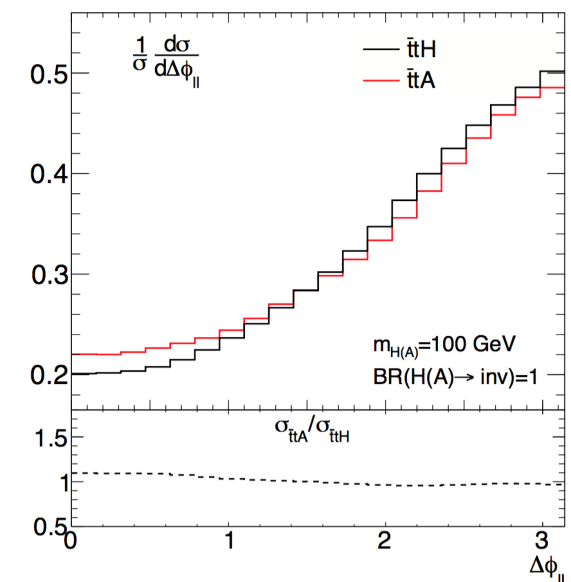

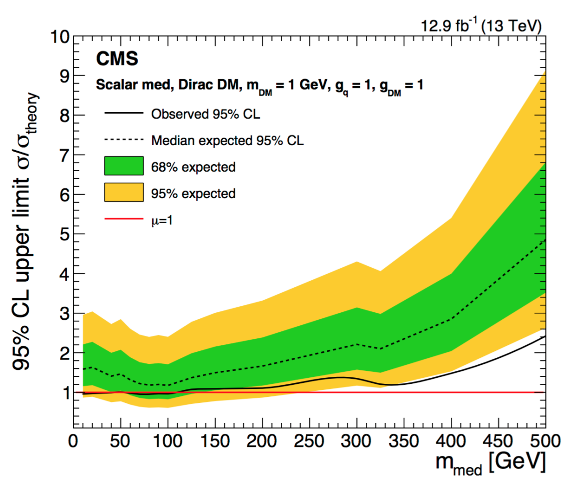

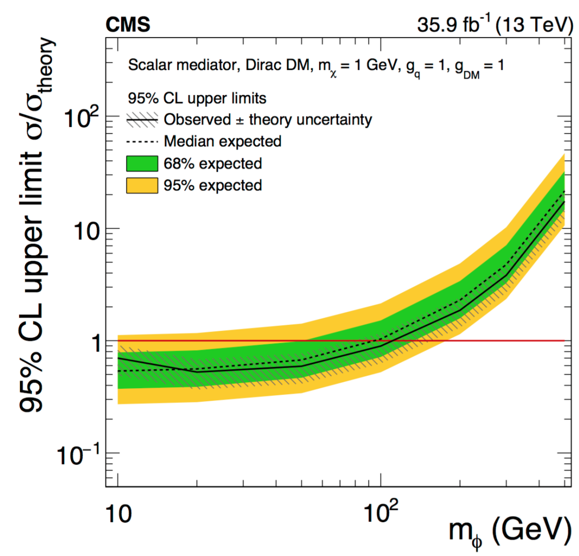

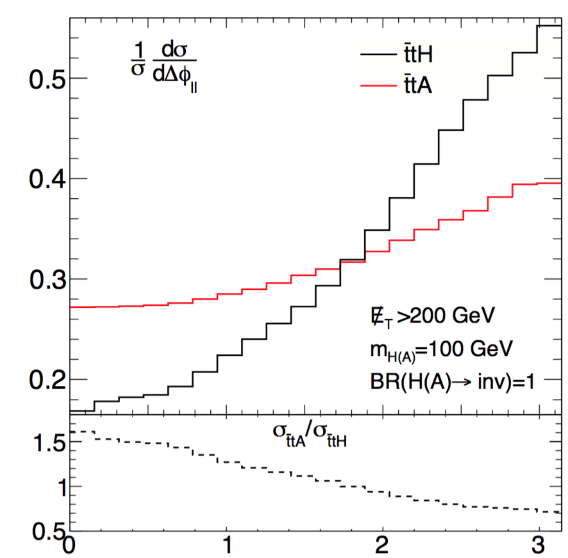

CMS mono-jet search, arXiv:1703.01651

CMS tt+DM search in dileptonic channel, arXiv:1711.00752

Signal and Bkgd

The dominant DM production process:

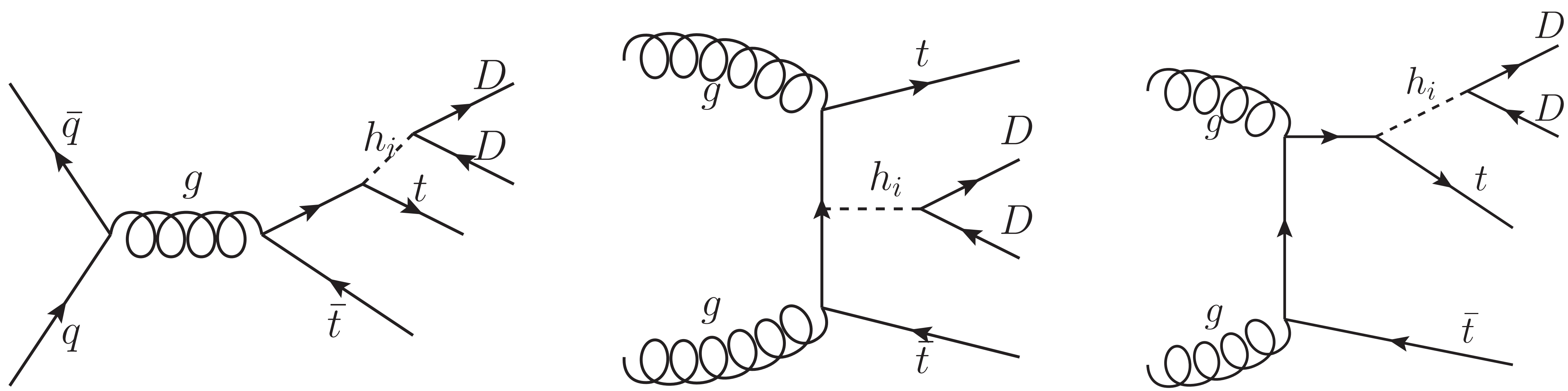

Dominant background processes:

	Cross section (NLO)
$\bar{t}t$	1316.5 pb
$\bar{t}tW$	20.5 pb
$\bar{t}tZ$	64.2 pb

	$t(\to b\ell\nu)t(\to b\ell\nu)+$ DM
FDM200	34.2 fb
FDM300	18.7 fb
FDM400	14.8 fb
FDM500	12.5 fb

Features of DM spin

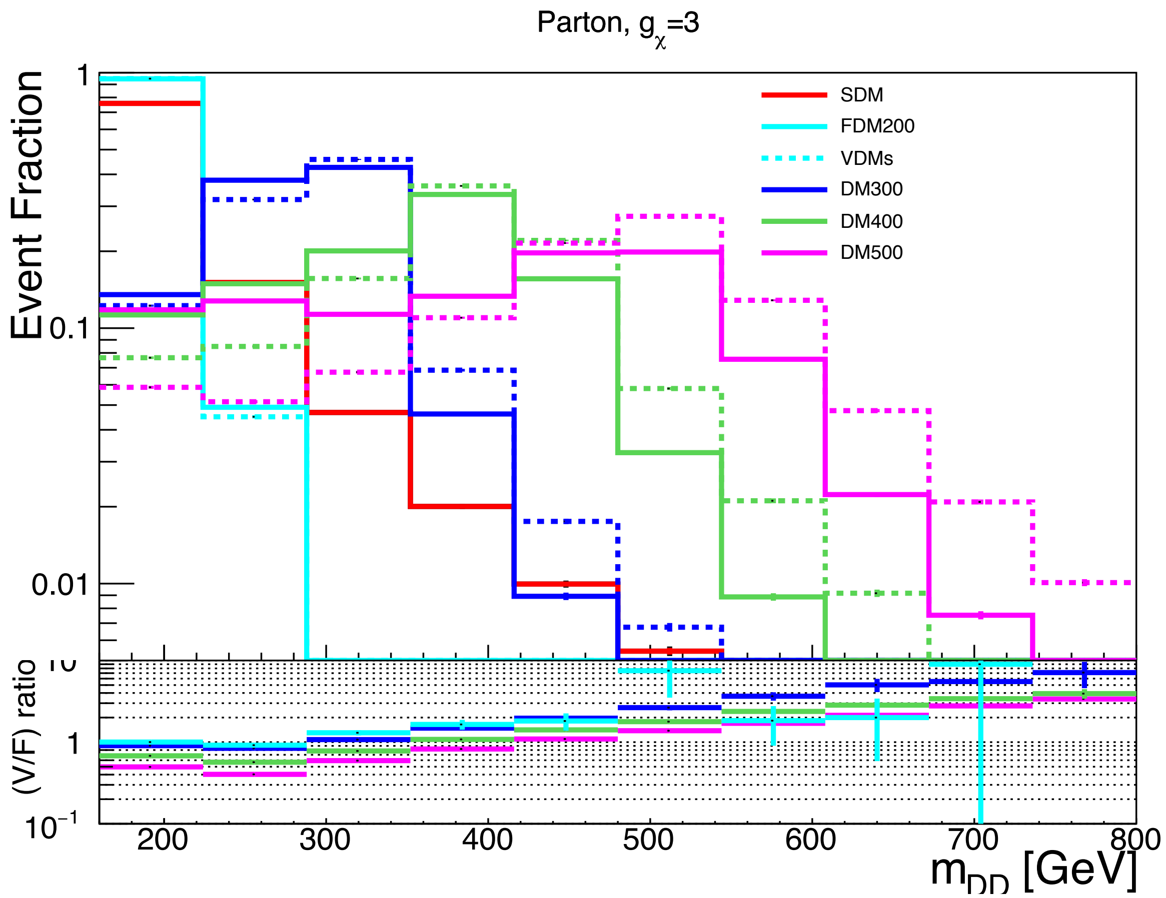

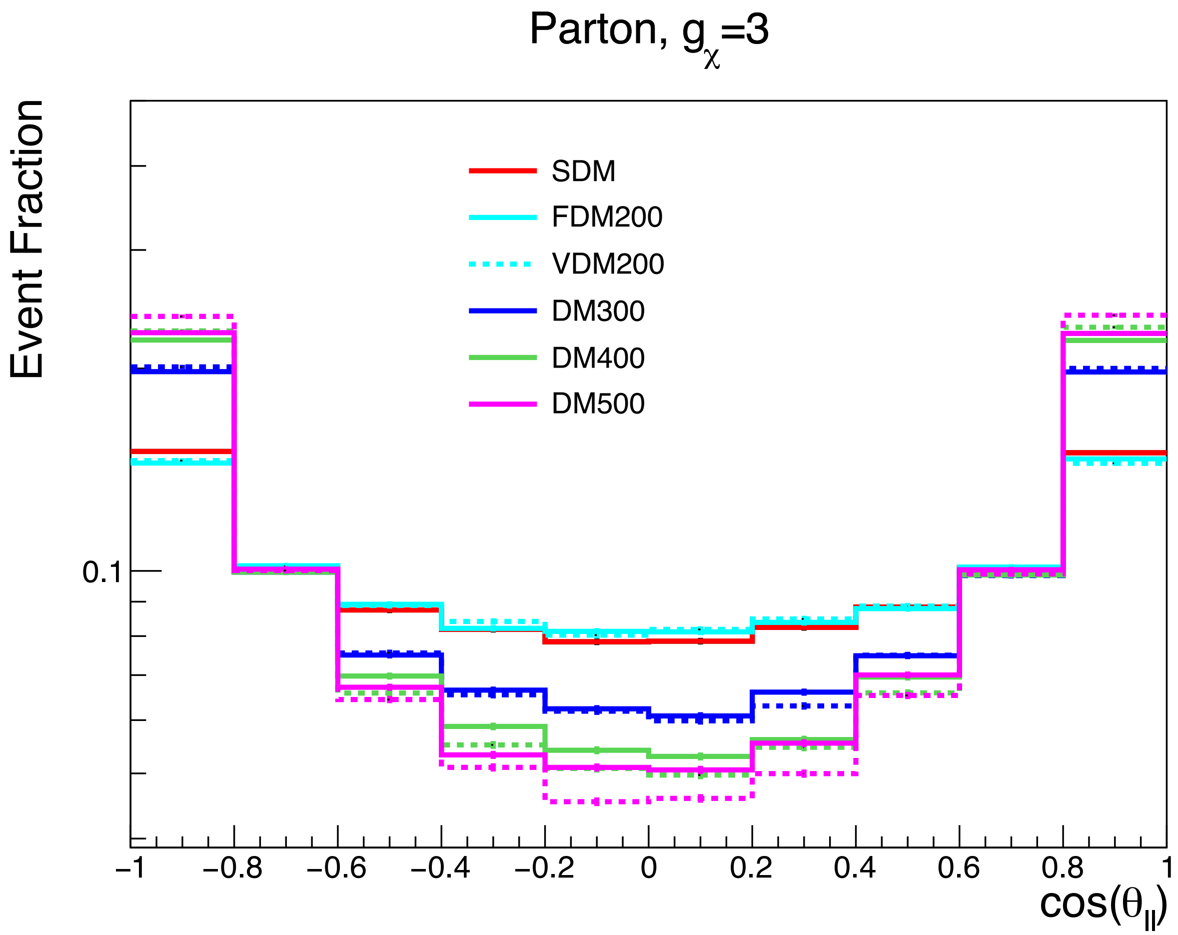

Analysis Strategy

- Preselection: Exactly two opposite sign lepton and at least one b jet in the final state.
- $m_{\ell\ell} \notin [85, 95]$ GeV.

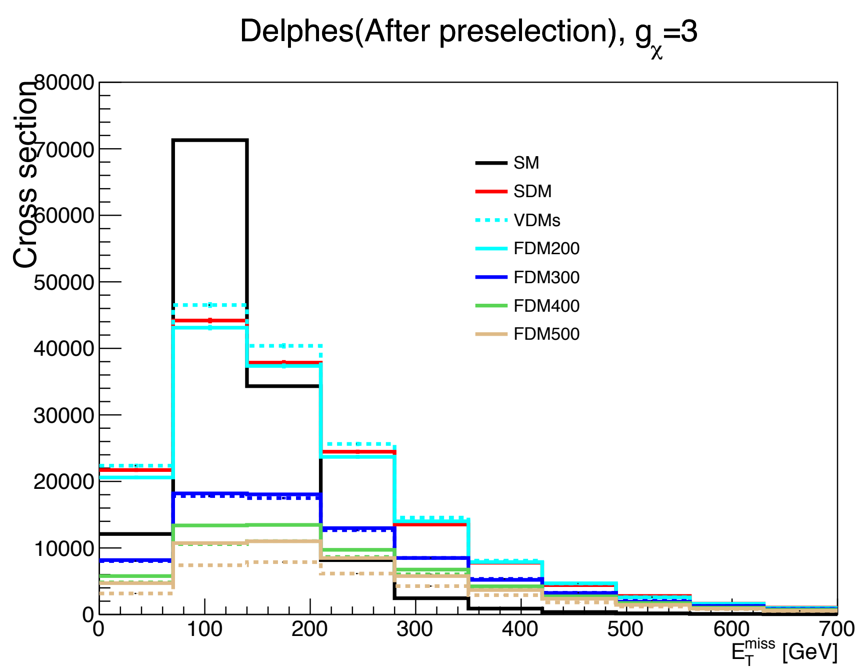

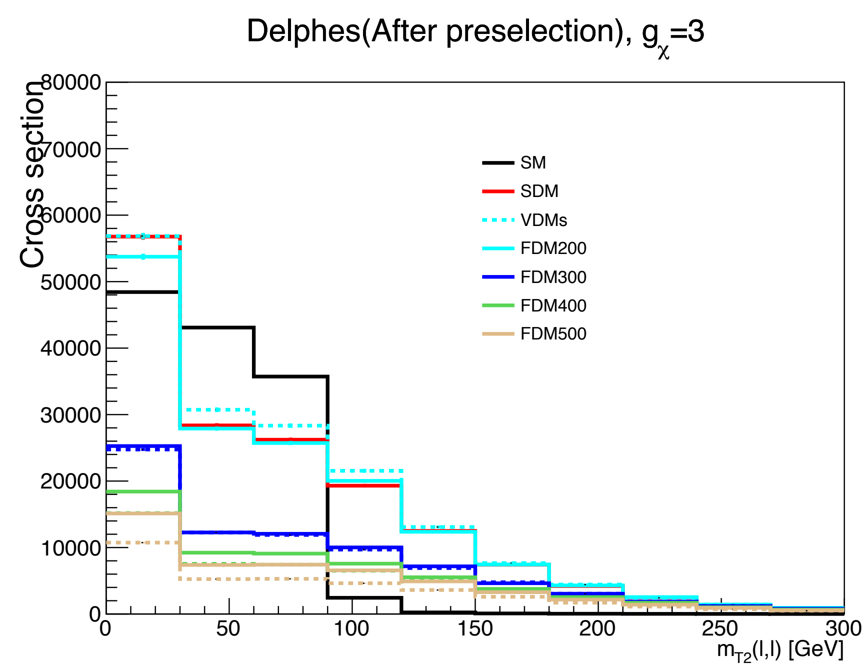

- $E_T^{miss} > 150$ GeV.
- $m_{T_2}(l, l) > 150$ GeV.

Cuts flow for SM processes and signals

Backgrounds Cross section	$\bar{t}t$ 1316.5 pb	$\bar{t}tW$ 20.5 pb	$\bar{t}tZ$ 64.2 pb
Presections	63.76 pb	351.8 fb	1.9 pb
$m_{\ell\ell} \notin [85, 95]$ GeV	59.8 pb	330.4 fb	1.05 pb
$E_T^{miss} > 150$ GeV	17.76 pb	69.61 fb	261.14 fb
$m_{T_2}(l, l) > 150$ GeV	23.83 fb	1.92 fb	32.1 fb

Signals Cross section	FDM200 34.2 fb	FDM300 18.7 fb	FDM400 14.8 fb	FDM500 12.5 fb
Presections	7.86 fb	3.99 fb	3.05 fb	2.55 fb
$m_{\ell\ell} \notin [85, 95]$ GeV	7.47 fb	3.82 fb	2.92 fb	2.44 fb
$E_T^{miss} > 150$ GeV	4.17 fb	2.44 fb	1.93 fb	1.63 fb
$m_{T_2}(l, l) > 150$ GeV	0.87 fb	0.62 fb	0.54 fb	0.47 fb
$\mathcal{L}^{95\%}$ [fb^{-1}]	305	602	793	1047

Discovery prospects

Binned log-likehood analysis:

$$\mathcal{L}(\mathrm{data}|\mathcal{H}_\alpha) = \prod_i \frac{t_i^{n_i} e^{-t_i}}{n_i!}, \quad \mathcal{Q} = -2\log\left(\frac{\mathcal{L}(\mathrm{data}|\mathcal{H}_\alpha)}{\mathcal{L}(\mathrm{data}|\mathcal{H}_0)}\right).$$

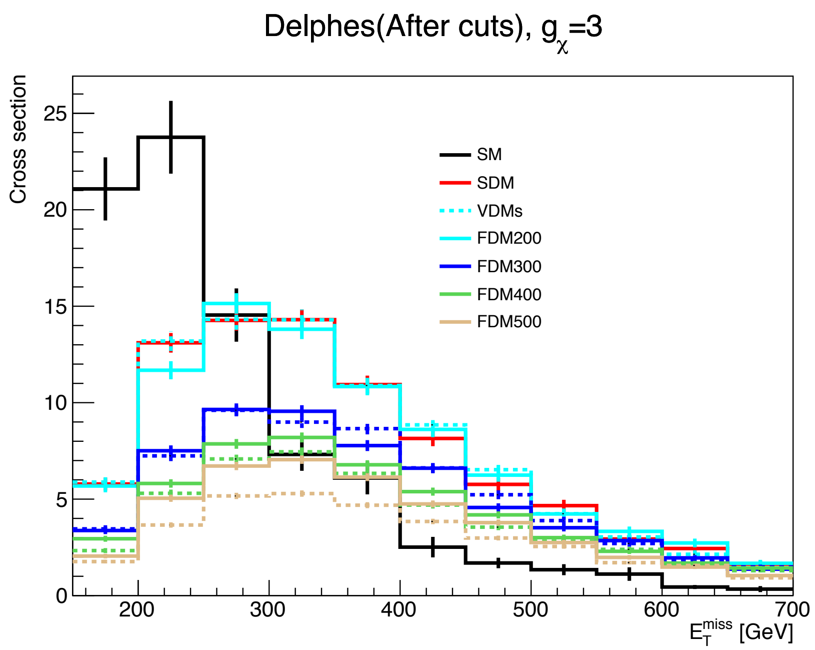

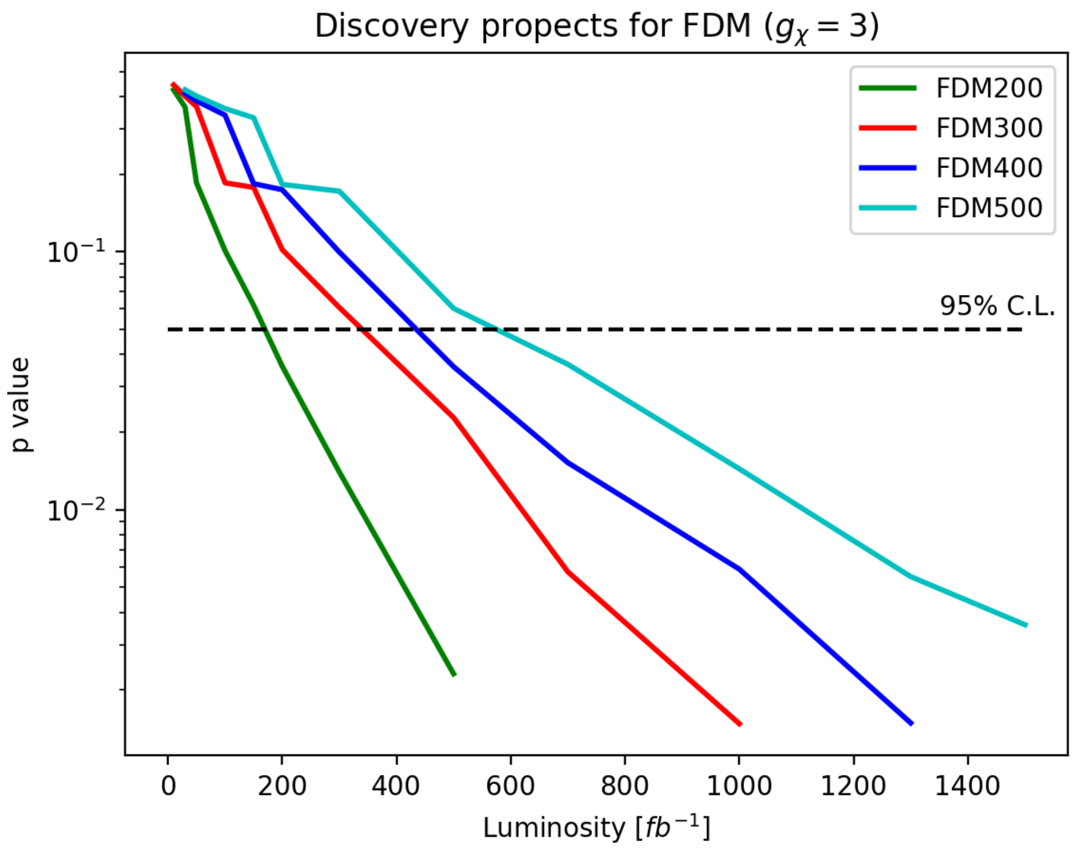

Spin characterization

Two dimensional binned log-likelihood test: $\mathcal{L}(\text{data}|\mathcal{H}_\alpha) = \prod_{i,j} \frac{t_{ij}^{n_{ij}} e^{-t_{ij}}}{n_{ij}!}$

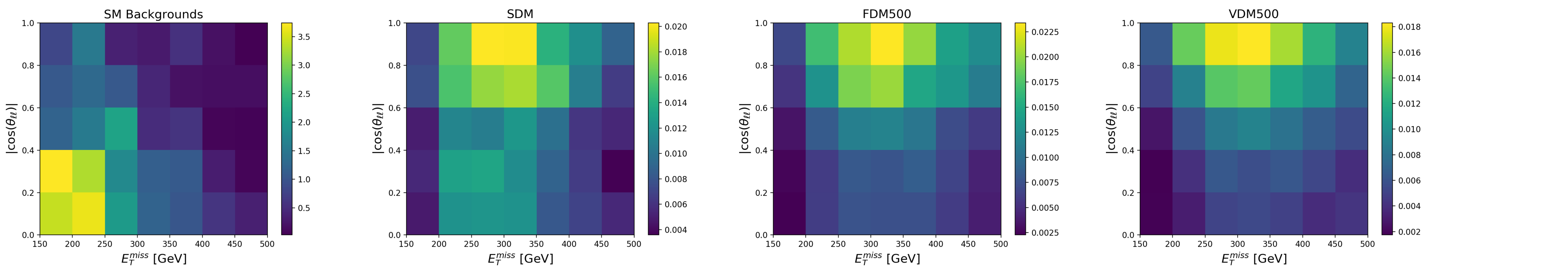

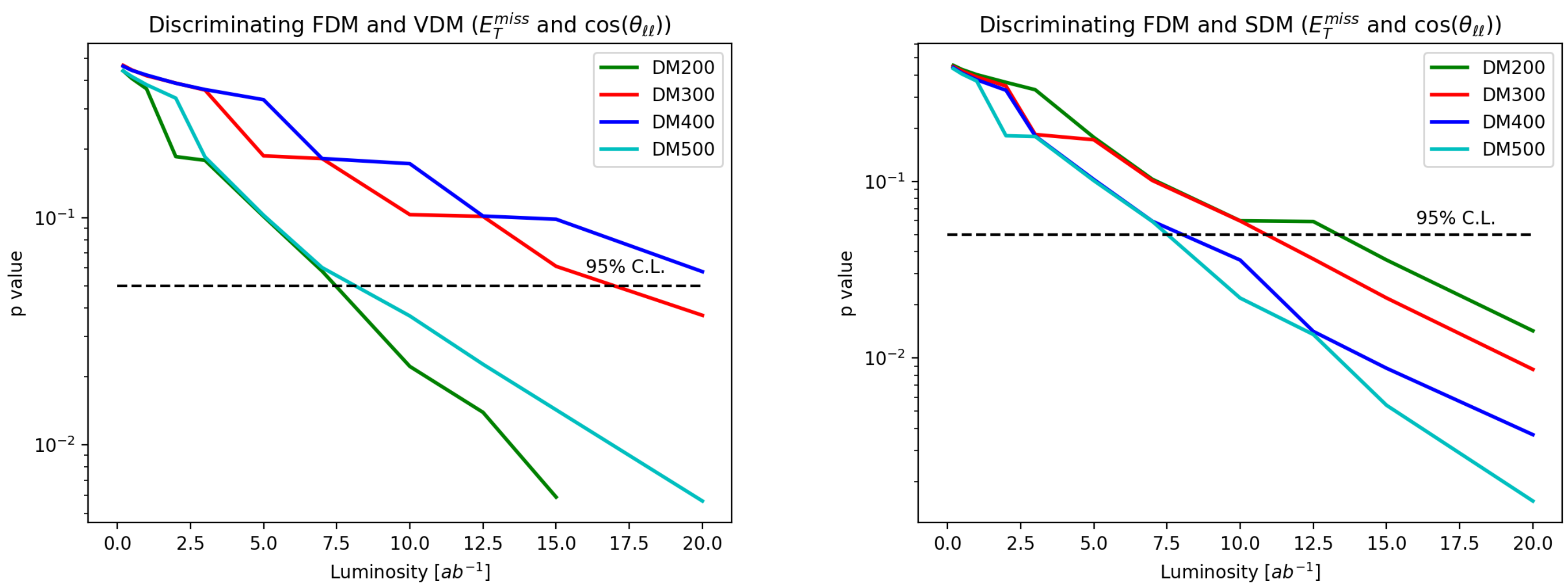

Summary

- The gauge invariant Higgs portal DM models for FDM and VDM require at least two mediators, while that of SDM only need one.
- At the ILC, $m_{H_2} \lesssim 300$ GeV can be probed at more than 3-σ level.
- At the 100 TeV p-p collider, (1)All benchmark points should be probable at integrated luminosity of $\mathcal{O}(100)$ fb^{-1} at 100 TeV p-p collider; (2) The spin discriminations for our benchmark points are possible at $\mathcal{O}(10)$ ab^{-1}. (3)Those values are all below the targets luminosity of FCC-hh, which is ~ 20 ab^{-1}.

Conclusion

- Renormalizable and unitary model (with some caveat) is important for DM phenomenology (EFT can fail completely)
- Imposing the full SM gauge symmetry is crucial for collider searches for DM
- Usually two propagators necessary for UV completion of the effective operators >> Important interference effects to be included in the data analysis

Backup

Benchmark points

- The relevant parameters in FDM for collider search:
  $g_\chi = 3,\ \sin\alpha = 0.3,\ m_\chi = 80$ GeV and $m_{H_2} = (200,\ 300,\ 400, 500)$ GeV.

$$\Gamma^{\rm FDM}_{\rm min}(H_2) = \Gamma(H_2 \to \chi\chi) + \Gamma(H_2 \to WW/ZZ) + \Gamma(H_2 \to ff)$$

$$= \cos^2\alpha \cdot g_\chi^2 \frac{m_{H_2}}{8\pi}(1 - \frac{4m_\chi^2}{m_{H_2}^2})^{3/2} + \sin^2\alpha \cdot \frac{G_\mu m_{H_2}^3}{16\sqrt{2}\pi}\delta_V \sqrt{1 - 4\frac{m_V^2}{m_{H_2}^2}}(1 - 4\frac{m_V^2}{m_{H_2}^2} + 12\frac{m_V^4}{m_{H_2}^4})$$

$$+ \sin^2\alpha \cdot (\frac{m_f}{v})^2 \frac{3m_{H_2}}{8\pi}(1 - \frac{4m_f^2}{m_{H_2}^2})^{3/2}\ ,$$

where f is the SM fermion, $V = Z, W$ and $\delta_V = 1(2)$ for $Z(W^\pm)$.

- Parameters for the vector DM production are chosen accordingly:
  $\sin\alpha = 0.3,\ m_V = 80$ GeV and g_V is chosen such that the total decay width of H_2 is the same as benchmark points of FDM.

m_{H_2} [GeV]	200	300	400	500
$\Gamma_{\rm min}(H_2)$ [GeV]	14.2	60.1	103.0	144.5
g_V	3.53	3.07	2.37	1.91

- Fix $m_S = 80$ GeV and take appropriate λ_{HS} such that the production cross section of the signal process is the same with that in the FDM.

Discovery prospects of the hadronic channel

Kinematic distributions:

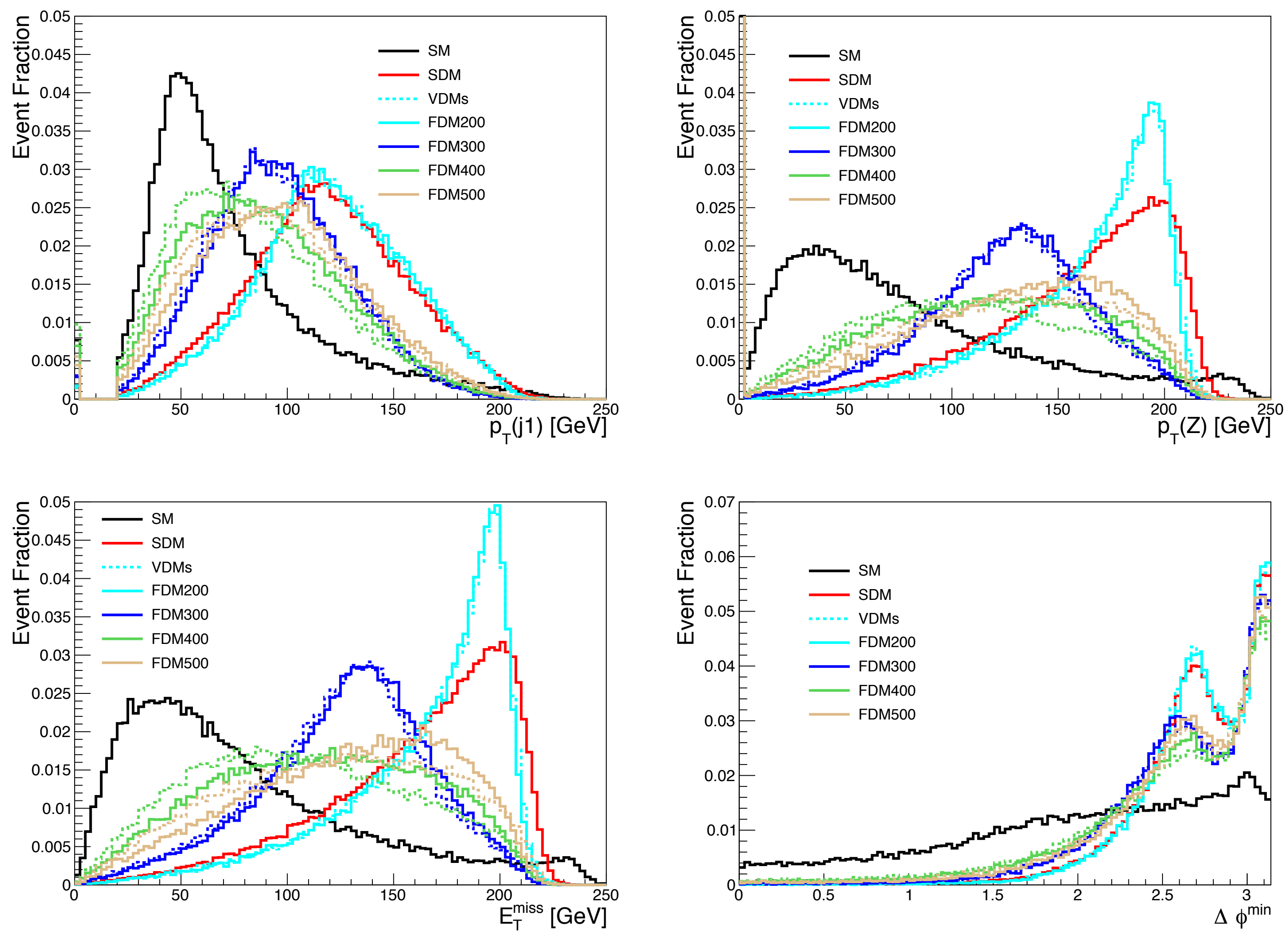

$$\Delta\phi^{\min} = \min_{i=1,2} \Delta\phi(p_T^{\text{miss}}, p(j_i))$$

Spin characterization

The same preselection and BDT cuts as used for FDM the benchmark point FDM200 (FDM300) are applied to the corresponding benchmark point SDM200 (SDM300) and VDM200 (VDM300).

	SDM200	SDM300	VDM200	VDM300
σ^0 [fb]	1.643	0.9214	1.734	0.8674
ϵ^{pre}	0.7875	0.7875	0.801	0.711
$N_S/1000\ \mathrm{fb}^{-1}$	447	322.3	726	363.5
$\mathcal{S}$	4.4	3.3	0.59	0.44

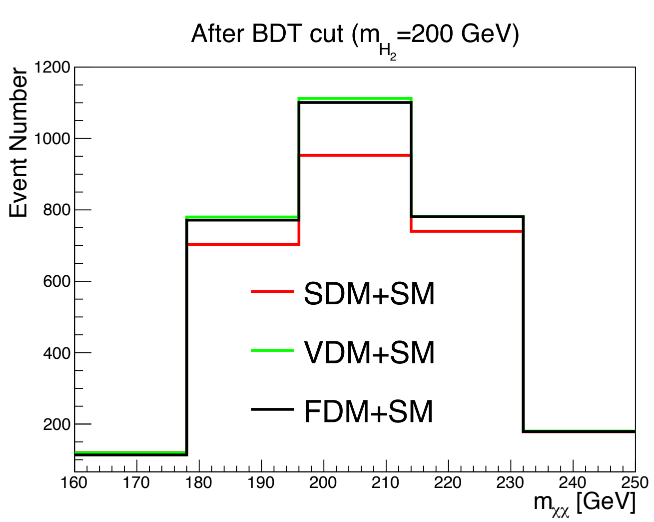

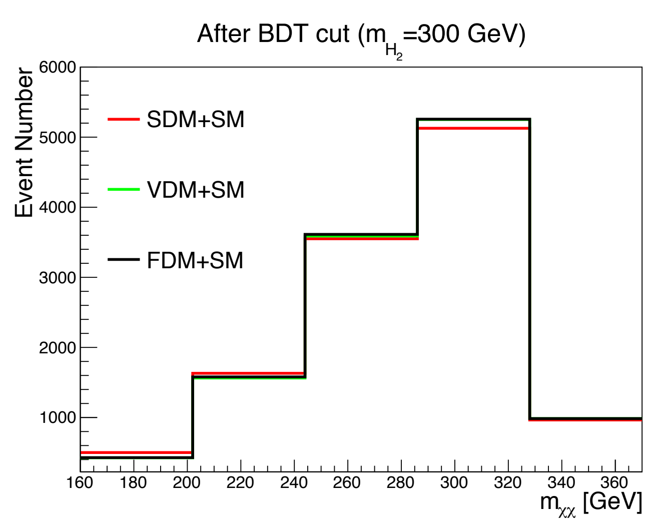

$$\mathrm{SDM:}\ \delta\chi^2 = \sum_{i=1}^{5}\Big(\frac{N_i^{\mathrm{FDM+SM}} - N_i^{\mathrm{SDM+SM}}}{\sqrt{N_i^{\mathrm{FDM+SM}}}}\Big)^2$$

$$\mathrm{VDM:}\ \mathcal{S} = |N_S^{\mathrm{FDM}} - N_S^{\mathrm{VDM}}|/\sqrt{N_B}$$

Spin characterization

Using only the distribution of E_T^{miss}:
$\mathcal{H}_0$ is the FDM + SM, $\mathcal{H}_\alpha$ can be VDM/SDM + SM